COMPDYN 2013
4th ECCOMAS Thematic Conference on
Computational Methods in Structural Dynamics and Earthquake Engineering
M. Papadrakakis, V. Papadopoulos, V. Plevris (eds.)
Kos Island, Greece, 12–14 June 2013

INFLUENCE OF LOW-CYCLE FATIGUE AND CORROSION PHENOMENA ON THE DUCTILE BEHAVIOUR OF STEEL REINFORCING BARS

A. Braconi[1], F. Braga[2], S. Caprili[3], R. Gigliotti[2], W. Salvatore[3]

[1] RIVA FIRE S.p.A
Viale Certosa 247, Milano (Italy)
e-mail: aurelio.braconi@rivagroup.com

[2] Dipartimento di Ingegneria Strutturale e Geotecnica, Università di Roma La Sapienza
Via Eudossiana 18, Roma (Italy)
e-mail: braga.franco@virgilio.it, rosario.gigliotti@uniroma1.it

[2] Dipartimento di Ingegneria Civile e Industriale, Università di Pisa
Largo L. Lazzarino 1, Pisa (Italy)
e-mail: silvia.caprili@ing.unipi.it, walter@ing.unipi.it

Keywords: Seismic demand, mechanical capacity, corrosion phenomena, Incremental Dynamic Analyses

Abstract. *Actual standards for constructions prescribe the realization of r.c. structures able to dissipate the energy stored during the earthquake through the development of global collapse mechanisms; the capacity design procedure is generally adopted, individuating specific "plastic hinges" in which the plasticization shall be located and using specific shear design actions opportunely over-dimensioned in order to avoid local brittle failures. The dissipative capacity of the structure is directly related to the rotational capacity of the elements in which plastic hinges are located and strictly depends on the geometrical and mechanical characteristics of the section itself and on the ductile capacity of steel reinforcing bars. The evaluation of the low-cycle fatigue behaviour of the rebars is obviously of relevant importance for the analysis of the structural behaviour of seismic r.c. buildings; two aspects shall be widely discussed, mainly related to the definition of the effective seismic demand on the rebars due to earthquakes and to the effective cyclic capacity of reinforcements. In the present work, developed inside the framework of a European research project called Rusteel (2009) the results coming from an accurate analysis of the seismic behaviour of r.c. structures is presented, evaluating, in particular, the effective level of strain and dissipated energy due to earthquake events on rebars. The mechanical characterization of the low-cycle fatigue behaviour of bars commonly used in r.c. buildings was also executed, leading to the comparison with the data coming from numerical analyses.*

1 INTRODUCTION

Reinforced concrete buildings in seismic areas are designed according to the capacity design (CD) approach, reference technique for anti-seismic constructions adopted by actual International standards [1, 2, 3]. Buildings shall be able to satisfy the deformation requirements due to increasing levels of seismic action without the exhibition of significant losses of strength and stiffness. Modern codes allow the development of significant plastic phenomena in specific structural elements during severe seismic excitations, causing the deterioration of the structural properties especially if deformations overpass the elastic limit. The failure of primary structural elements, as a consequence, can happen for strain levels lower than the ones corresponding to the collapse limit, condition generally known as "low-cycle fatigue" [4].

In the case of reinforced concrete (r.c.) buildings, in particular, the ability to dissipate the seismic energy stored during the earthquake is strictly connected to the development of global collapse mechanisms, and depends on an opportune location of plastic phenomena: plastic hinges, in the case of moment resisting frames (MRF), generally coincide with the ends of primary elements, following the scheme weak beams – strong columns. Elements shall present an adequate ductility level to prevent unexpected brittle failures and to globally dissipate seismic energy. Since the development of plastic hinges depends on the rotational capacity of primary structural elements [5], a deep knowledge of the cyclic response of the steel reinforcing bars in correspondence of plastic hinges is required to correctly understand the structural behaviour of r.c. buildings under seismic action.

Many works were presented in the current literature dealing with the evaluation of the effective seismic demand on different kinds of structures and sub-structures [4, 6, 7, 8, 9, 10, 11, 12] but in general, no information were provided about the effective ductility demand on steel reinforcing bars, in terms of both strain level and energy dissipation. In their work, Barrera et al. [13] presented the results of experimental tests executed on r.c. columns considering both vertical axial load and a monotonic increasing lateral force. Results were reported including the minimum and maximum strain levels on steel bars: nevertheless, also in this case, a detailed investigation of the cyclic behaviour of bars was not provided, with results limited to the monotonic condition.

Despite a large scientific literature about the cyclic structural behaviour of reinforced concrete buildings, few information are actually provided regarding the Low-Cycle Fatigue (LCF) performance of steel reinforcements, resulting in the absence of a specific procedure for the production control of the cyclic/seismic behaviour of steel bars to be used in modern buildings. Such problem is confirmed by the actual scenario of European standards for reinforcing steels, in which Mandate M115 *("Execution of standardisation work for harmonized standards on Reinforcing and prestressing steel for concrete")* of European Commission, in the framework of the revision of European standard EN10080:2005 [14], promoted the elaboration of a common protocol for the execution of LCF tests for the production control of steel reinforcing bars. Even if in some European Countries current standards for reinforcing steels include the LCF protocols (as, for example, Spanish code UNE 36065 EX:2000 [15] and Portuguese code LNEC E455-2008 [16]), such protocols are defined on the basis of empirical considerations, lacking any reliable background study. The lack of a codified procedure for LCF tests on steel bars is well evidenced in the current literature: Mander et al. [17], Brown and Kunnath [18], Crespi [19] executed LCF tests using levels of imposed deformation, testing frequencies and imposed number of cycles without any regard to the effective real earthquake demand.

Moreover, beside the problems already presented regarding the mechanical

characterization of the low-cycle fatigue/seismic behaviour of steel reinforcing bars, several works in the current literature [20] evidenced durability problems of TempCore bars in r.c. buildings located in aggressive environmental conditions (i.e. chloride exposition), with the decrease of their mechanical properties, both in terms of strength (yielding and tensile stress, R_e and R_m) and ductility (A_{gt}). In order to avoid such problems, Eurocode 2 [21] prescribes the adoption of an opportunely sized concrete cover in relation to the exposition class of the building and to the strength class of the concrete used in the design. Anyway, the knowledge of the mechanical behaviour of rebars after corrosion is necessary for the understanding of the monotonic and the cyclic/seismic behaviour of buildings and to evaluate the ability of the actually used reinforcing steels in sustaining the seismic ductile requirements also after corrosion attacks.

The present paper was developed in the framework of a European research project funded by the Research Fund for Coal and Steel (RFCS), Rusteel, *Effects of Corrosion on Low-Cycle Fatigue (Seismic) Behaviour of High Strength Steel Reinforcing Bars, 2009-2012* [22].

The main aim of the presented work consists in the evaluation of the seismic ductile demand (D) on steel reinforcing bars due to real earthquake events with respect to their effective ductile capacity (C), analyzed both in uncorroded and in corroded conditions.

In this way, the assessment of the structural behaviour of r.c. structures, representative of the actual scenario of European constructions, both at a global level and also considering the local hysteretic behaviour of steel reinforcing bars will allow the full knowledge of the structural response of selected buildings under natural seismic events of magnitude compatible with the one assumed during the design. Moreover, the ability of the actual European steel production usually adopted for new constructions to satisfy the ductile requirements imposed by earthquakes will be deeply investigated, taking into account the ability of corroded steel reinforcing bars, opportunely subjected to accelerated corrosion tests in salt spray chamber, to still satisfy the ductile requirements of seismic action, in terms of both deformation and energy dissipation.

2 THE ADOPTED METHODOLOGY

The main aim of the present work consists in the evaluation of the seismic ductility demand on steel reinforcing bars in r.c. structures and in the comparison of obtained results with the effective mechanical properties of bars, in terms of strain and dissipative capacity, both in uncorroded and corroded conditions.

In order to obtain the values of the effective levels of deformation and energy dissipation, Incremental Dynamic Analyses (IDA) shall be executed on non linear models of r.c. buildings representative of the actual scenario of European constructions.

Non linear bi-dimensional plane frame models of r.c. buildings characterized by different functional destinations (i.e. residential, commercial and office buildings), different plans and elevation dispositions (i.e. span length, interstorey height, number of spans), different ductility classes (High Ductility Class – HDC and Low Ductility Class – LDC) and designed following the prescriptions imposed by European and Italian standards (EN 1998-1:2005, D.M. 14/01/2008) for a peak ground acceleration (PGA) equal to 0.25g, were realized using OpenSees software [23].

The elaboration of the non linear models for the execution of IDAs required the individuation of a specific constitutive stress-strain law for steel reinforcements, allowing the correct evaluation of the levels of deformation and dissipated energy density due to earthquake events. Many works in the current literature [24, 25, 26], in fact, evidenced the inadequacy to consider full bond models for the representation of the hysteretic behaviour of r.c. components once that yielding is overpassed, due to significant relative slips between

steel and concrete, that cannot consequently be neglected.

The hardening slip model, based on the formulation by Braga et al. [25] and implemented to include hardening phenomena of steel reinforcements [27], was consequently developed and adopted for numerical simulations.

In order to maximize the seismic ductility demand on steel reinforcing bars and to reduce the time of analysis, specific accelerograms were selected from the European Strong Motion Database (ESMD), in relation to their PGA, number and the amplitude of cycles, to be used in the numerical IDA simulations. The maximization of the ductility demand on each designed building was developed through the adoption of an opportune procedure aiming to evaluate the Park and Ang (1989) damage index (DI_{PA}), taking into account the effects of seismic input in terms of both deformation (global displacement) and energy dissipation. The results of IDA simulations were then analyzed considering both the whole structure and the corresponding development of ductile and brittle mechanisms in relation to actual standards' prescriptions [1, 2], and the seismic/cyclic behaviour of steel reinforcing bars, in terms of stress, strain and dissipated energy (seismic demand, D).

For what concerns, on the other hand, the evaluation of the effective mechanical capacity (C) of steel reinforcing bars, experimental tensile and LCF tests were executed on a set of steel reinforcements representative of the actual European production, following a specific protocol elaborated inside the research project. Results of LCF tests were analyzed in terms of deformation and, in particular, energy dissipation in order to be comparable with the numerical data coming from IDAs.

Moreover, for taking into account the effects of corrosion phenomena on the mechanical behaviour of bars, accelerated corrosion tests in salt spray chamber were executed on a reduced set of specimens following a specific protocol elaborated inside Rusteel project; the corroded specimens were then subjected to both tensile and LCF tests, evaluating the modifications induced by corrosion on the mechanical behaviour of bars.

The comparison between demand (D) and capacity (C) allowed the assessment of the ability of actual European steel reinforcements' production to effectively satisfy the mechanical requirements induced by seismic events.

Figure 1 shows a schematic representation of the methodology adopted for the individuation of the effective ductile demand on reinforcements while Figure 2 presents the flowchart of the methodology adopted for the investigation of the capacity of bars.

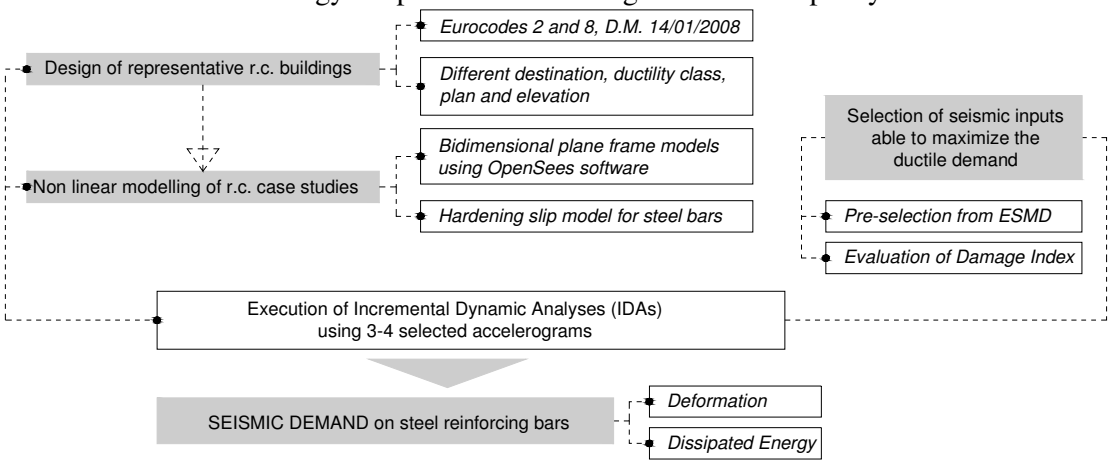

Figure 1: Flowchart for the definition of the effective seismic ductility demand on reinforcements.

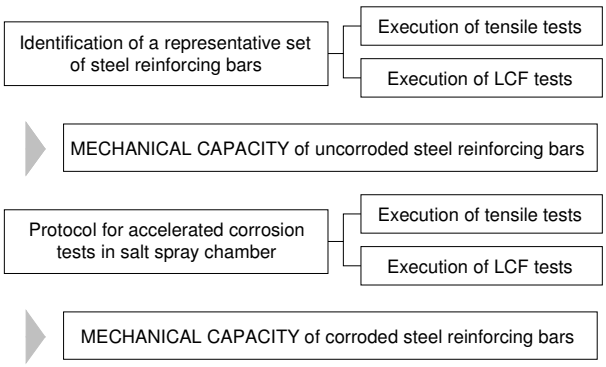

Figure 2: Flowchart for the definition of the effective seismic ductility capacity on reinforcements.

3 SELECTION AND DESIGN OF REPRESENTATIVE R.C. BUILDINGS

Reinforced concrete case-study buildings were designed following the prescriptions imposed by European and Italian standards for constructions [1, 2, 21]. Different distributions of structural elements, different functional destinations (commercial, residential and office buildings) and two different ductility classes (high ductility class – HDC and low ductility class – LDC) were considered.

Permanent gravitational loads were defined in relation to the typology of structural and not structural elements (storey slabs, roof, internal and external infills, equipments, etc…), while live loads were defined in relation to the functional destination selected and according to what specified by Eurocode, according to what presented in table 1.

The response spectrum adopted for the characterization of seismic action was defined in relation to Italian standard prescriptions [2], more restrictive than the one adopted by Eurocode 8: two different limit state, i.e. Life Safety limit state (LS), as regards strength, and Damage Limitation limit state (DL), as regards stiffness and displacements, were adopted, with corresponding return periods (T_R) respectively equal to 75 and 475 years respectively. Buildings were consequently designed using a peak ground acceleration (PGA) equal to 0.25g for LS and considering soil category B. For moment resisting frame (MRF) structures behaviour factors respectively equal to 3.90 and 5.85 for LDC and HDC were adopted [1, 2]. Steel grade B450C and concrete class C25/30 were used. Table 2 summarizes the main aspects assumed in the design phase.

Functional Destination	Ductility Class	Structural loads (kN/m^2)	Not structural loads (kN/m^2)	Q (kN/m^2)
Residential	HDC	3,35	2,80	2,00
Residential	LDC	3,35	2,80	2,00
Office	HDC	3,70	2,50	3,00
Commercial	HDC	4,00	2,35	5,00

Table 1: Loads adopted for the design of r.c. representative buildings.

Functional destination	PGA [g]	Ductility class	Steel grade	q factor
Residential building	0,25	HDC	B450C	5,85
Residential building	0,25	LDC	B450C	3,90
Commercial building	0,25	HDC	B450C	5,85
Office building	0,25	HDC	B450C	5,85

Table 2: Designed reinforced concrete case studies.

MRFs with span length of beams variable between 4.0 m and 7.0 m and storey height between 2.5 m and 5.0 m were adopted in relation to the functional destination of the buildings. Residential buildings in both HDC and LDC presented the same geometrical arrangement of structural elements, resulting in an area of 60,0x14,0 m^2 and a total height of 14,0 m (figure 3); commercial building in HDC was characterized by an area of 36,0x34,0 m^2 and a total height of 19,0 m (figure 4) and, finally, office building in HDC presented an area of 108,0x30,0 m^2 and a global height of 19,0 m (figure 5).

Tridimensional linear models were elaborated using SAP 2000 (v.14.1) software for the execution of linear modal analysis; in the linear models, mono-dimensional elements were used for both beams and columns, while for the slabs of the stairs two-dimensional plane "shell" elements were adopted to directly take into consideration the stiffening contribution of stairs and lift's rooms. The storey slabs were modeled introducing a rigid diaphragm in correspondence of each floor, since a concrete slab with reinforcement grid of 40 mm of thickness was adopted according to the design; columns were fixed at the base.

For taking into account the cracking phenomena of concrete at LS limit state, a reduction of the stiffness of primary structural elements (beams and columns) was adopted, according to what presented in the current standards and literature [1, 2, 5]: a reduction of stiffness equal to 50% was adopted for beam elements and a reduction of stiffness equal to 30% was adopted for column elements, characterized by a significant axial load, for all the designed buildings.

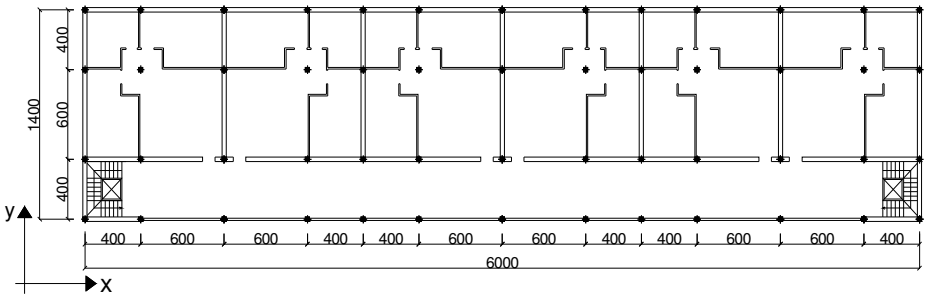

Figure 3: Geometrical scheme adopted for residential buildings.

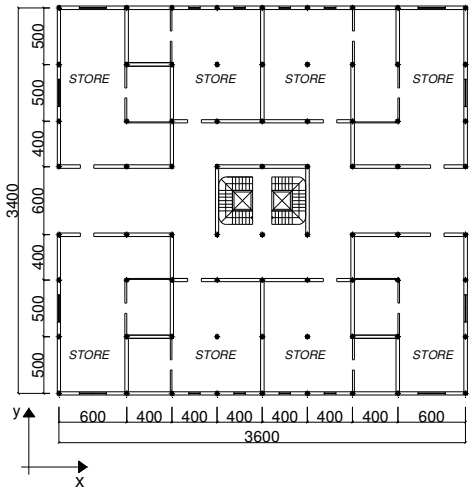

Figure 4: Geometrical scheme adopted for commercial building.

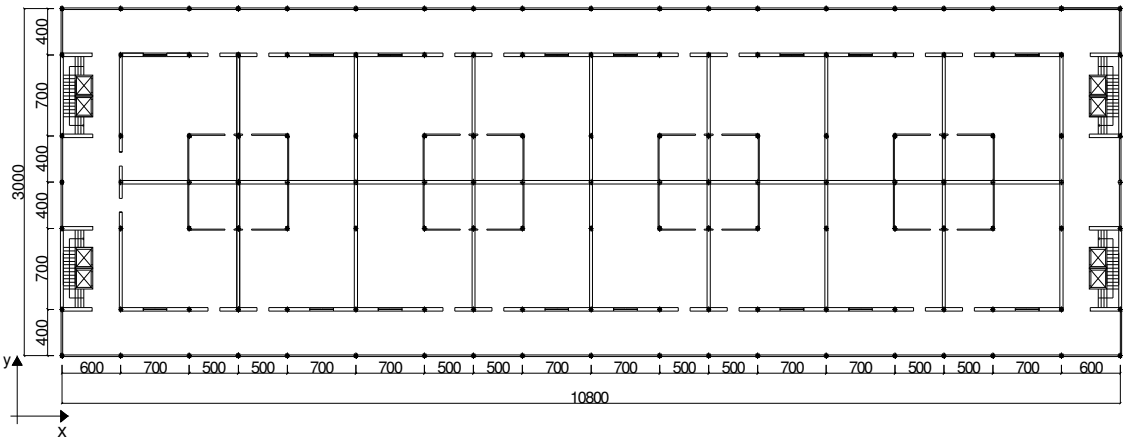

Figure 5: Geometrical scheme adopted for office building.

4 ELABORATION OF NON LINEAR MODELS OF R.C. BUILDINGS

Non linear bi-dimensional plane models were elaborated for each of the two main directions of designed buildings using OpenSees software (Mazzoni et al. 2007). The validation of the adoption of plane frame models instead of tri-dimensional ones was widely presented in Caprili [27] and Braconi et al. [28].

Beams and columns were modelled as "beam with hinge" (BWH) elements: each single element was divided into three different portions, two plastic hinges in correspondence of the two ends and an elastic central part (figure 6). The definition of the section in correspondence of the central part of the element required only the individuation of the transversal area (A) and of the elastic modulus of material (E_m); on the other hand, the sections in correspondence of the two ends of beams and columns were modeled as "fibre section" and an opportune plastic hinge length (L_p) was defined according to Panagiotakos and Fardis's formulation [29] for cyclic loading condition:

$$L_{pl,cy} = 0.12 \cdot L_s + 0.014 a_{sl} d_b f_y \tag{1}$$

Being L_s the shear span length, a_{sl} a coefficient for slip equal to 1 if there is slippage of the longitudinal bars from their anchorage beyond the section of maximum moment, or to 0 if there is not slip, d_b is the bar diameter and f_y the yielding strength. In the present work, the value of a_{sl} was assumed equal to zero, since the relative slip phenomena between bars and the surrounding concrete was directly taken into consideration in the adopted hardening slip model. Columns were fixed at the base and seismic masses, evaluated according to Eurocode 8 [1], were concentrated in correspondence of the top of the columns, where vertical loads were also applied. In order to reproduce the stiffening contribution of storey slabs, additional truss elements, opportunely sized, were introduced in the model between columns (figure 6).

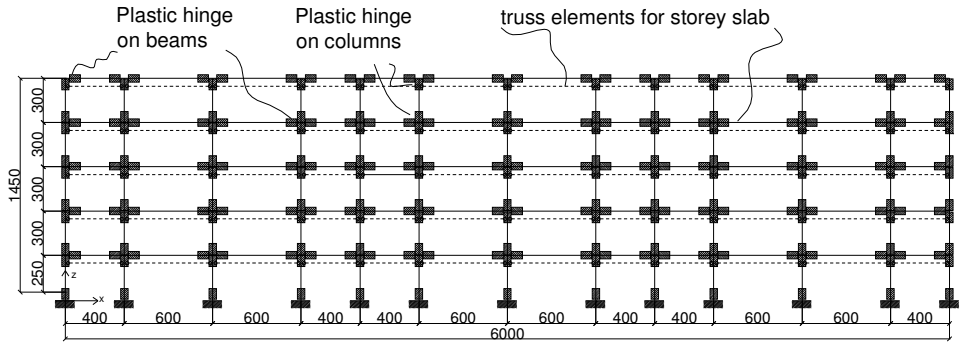

Figure 6: Simplified scheme of non linear model with beam with hinges elements (residential building).

For concrete material, the constitutive law proposed by Braga, Gigliotti and Laterza (BGL) [31] was used, able to directly represent the confinement contributions due to both longitudinal and transversal reinforcements.

For steel reinforcing bars, the "hardening slip model", widely presented in [27, 28], was adopted to represent the effects of relative slips between steel reinforcements and concrete. The hardening slip model was implemented in OpenSees using the trilinear hysteretic material [23], with the three characteristic points of the loading envelope opportunely determined in relation to the energy equivalence principle (figure 7), as well as already presented in [25].

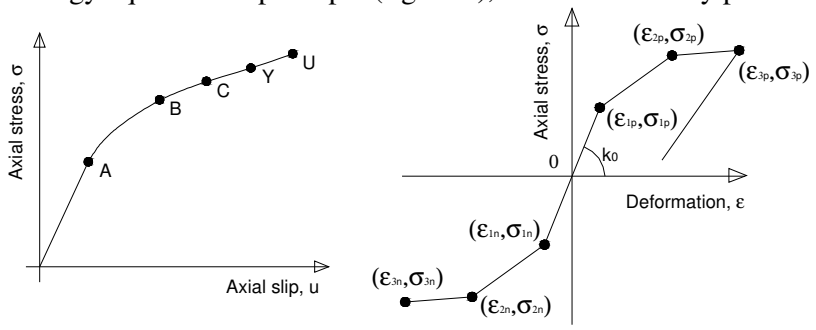

Figure 7: Shift from axial stress-slip model to axial stress-fictitious strain model for steel bars.

The following assumptions were made for the elaboration of the hardening slip model to use for steel reinforcing bars (figure 8):

- The constitutive stress-slip relationship was assumed elastic-plastic with hardening and the values adopted for yielding (f_y) and tensile strength (f_u) and for the elongation to maximum load (A_{gt}) were calibrated on the base of the mean values of the experimental tests' results on steel reinforcements B450C [29] and were respectively equal to 490 MPa, 600 MPa and 14.0%.
- The bond stress-slip relationship was assumed elastic-perfectly plastic (figure 8). The values provided by Model Code 90 [31] for ribbed bars were assumed; in order to consider the progressive deterioration and damaging of bond between steel and concrete due to cycling actions, the residual bond stress to use in the model (τ_d) was taken equal to the one prescribed for poor bond conditions in confined concrete (table 3). A linear approximation of the first branch between zero and the point with coordinates (u1, τ_d) was adopted (figure 8).

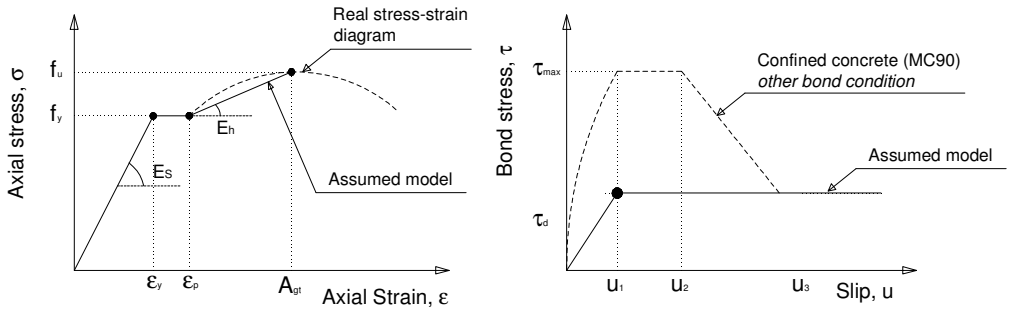

Figure 8: Assumed relationships for stress-strain constitutive law and for bond stress-slip law.

Confined concrete - All other bond condition			
Model Code 90 (CEB-FIP 1993)		Assumed values for modified slip model	
u_1 [mm]	1.0	u_b [mm]	0.4
u_2 [mm]	3.0	u_2 [mm]	-
u_3 [mm]	Clear rib spacing	u_3 [mm]	-
α	0.4	f_{ck} [MPa]	33
τ_{max} [MPa]	$1.25\sqrt{f_{ck}}$	τ_{max} [MPa]	7.18
τ_f [MPa]	$0.40\tau_{max}$	τ_f [MPa]	2.87

Table 3: Assumed values for the bond stress-slip relationship in modified slip model.

The axial stress-strain to be used in the numerical models was obtained according to what provided by D'Amato et al. [32]; a fictitious strain ε^* was individuated through the following equation:

$$\varepsilon^* = \frac{u_{L,tot}}{L_P} \tag{2}$$

in which the plastic hinge length L_p was defined according to Panagiotakos and Fardis [29]. Figures 9 represent the axial stress-slip and the axial stress-strain trilinear relationships obtained for different bar diameters, while table 4 summarizes the values adopted in the models.

Mechanical properties of material			Axial stress-slip relationships: coordinates of significant points								
f_y	490	MPa									
f_u	600	MPa	d	14	mm	d	16	mm	d	18	mm
ε_y	0.24	%	u_{p1}	0.400	mm	u_{p1}	0.400	mm	u_{p1}	0.400	mm
A_{gt}	12.50	%	σ_{p1}	318.56	MPa	σ_{p1}	297.80	MPa	σ_{p1}	280.77	MPa
E_s	206000	MPa	u_{p2}	0.743	mm	u_{p2}	0.839	mm	u_{p2}	0.936	mm
E_h	1047.00	MPa	σ_{p2}	517.30	MPa	σ_{p2}	517.44	MPa	σ_{p2}	517.59	MPa
τ_d	2.87	MPa	u_{p3}	11.475	mm	u_{p3}	13.104	mm	u_{p3}	14.734	mm
u_1	0.4	Mm	σ_{p3}	600.00	MPa	σ_{p3}	600.00	MPa	σ_{p3}	600.00	MPa

Table 4: Assumed values for the axial stress-slip model.

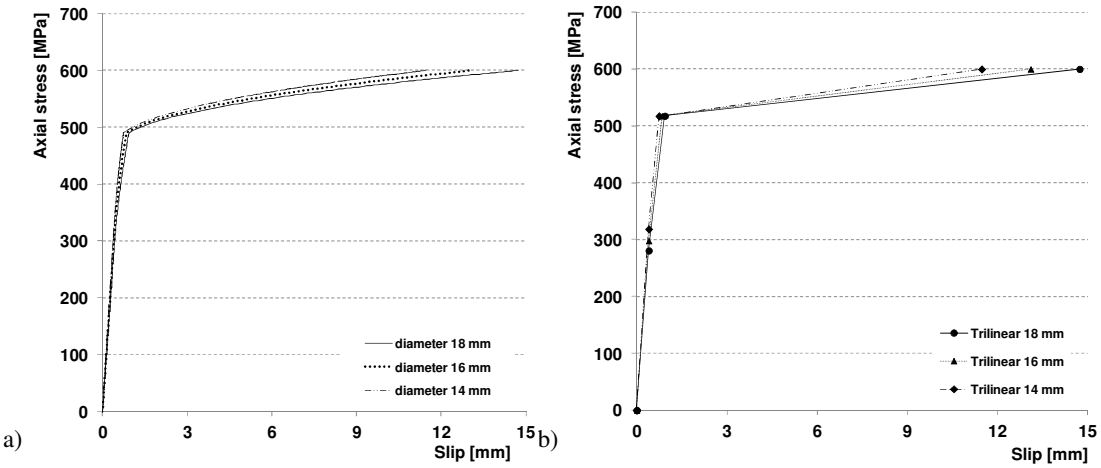

Figure 9: a) Axial stress-slip relationship and b) trilinear equivalent model.

5 GLOBAL ASSESSMENT OF CASE STUDIES

IDAs were executed on bi-dimensional frame models considering both the horizontal and the vertical components of accelerograms and PGA increment equal to 0.05g; the adopted time histories, selected from the European Strong Motion Database (EMSD) in order to maximize the seismic ductile requirements on buildings according to the procedure specified in Braconi et al. [33] are presented in table 5.

Building	Time histories			
Residential HDC	Montenegro x+z	Erzincan x+z	Campano Lucano x+z	Umbro Marchigiano x+z
Residential LDC	Montenegro x+z	Erzincan x+z	Campano Lucano x+z	Umbro Marchigiano x+z
Commercial	Montenegro y+z	Erzincan x+z	Campano Lucano y+z	Umbro Marchigiano x+z
Office	Montenegro y+z	Erzincan x+z	Campano Lucano y+z	Umbro Marchigiano x+z

Table 5: Adopted time histories for the IDAs.

The global structural assessments of designed buildings was executed following the prescriptions imposed by actual European and Italian standards [1, 2, 34]. The structural safety was checked at the member section level by comparing the demand, derived from numerical analyses, with its corresponding available capacity, evaluated in terms of strength or deformation respectively for brittle and ductile elements or mechanisms.

The ductile mechanisms were assessed evaluating the chord rotation demand and the corresponding capacity at the ends of each structural element (beams and columns); the brittle elements/mechanisms were assessed evaluating their strength capacity, in terms of static or cyclic shear resistance according to Eurocode 8.

The capacity of r.c. structural members at Damage Limitation limit state (DL) was expressed in terms of chord rotation at yielding θ_y, while the value of total chord rotation capacity (considering both the elastic and the inelastic parts) at ultimate (Near Collapse, NC) limit state were evaluated in agreement to what specified in the Annex A of Eurocode 8 [34]. For what concerns brittle elements/mechanisms, according to Eurocode 8 both the static and the cyclic shear capacity of elements were taken into account, since the effects of the inelastic response in the assessment of the shear capacity was necessarily taken into account decreasing the shear strength with the progressive increase of the cyclic inelastic deformations. The static

shear static strength was evaluated according to Eurocode 2 [21].

The cyclic shear resistance V_R was also evaluated at ultimate limit state (NC), according to the formula presented in the Annex A of Eurocode 8 (expression A.12 of [34]).

The results of numerical analyses on r.c. buildings designed in high ductility class (HDC) evidenced, in general, a good agreement with what imposed during the design, without the activation of shear mechanisms in beams and columns and the development of ductile ones for levels of PGA higher than the ones corresponding to the design one (0.25g). The reaching of the interstorey drift limit, equal to 4.0% according to [3], generally happened for PGA levels higher than 0.30g. Figures 10-12 represent the progressive activation of ductile mechanisms (chord rotation at yielding and ultimate) for increasing levels of seismic action for the three HDC buildings and for the most critical seismic event.

As visible, plastic hinges generally developed at the ends of beams of the first three levels and at the base of columns of the 1st floor, for increasing levels of seismic action: as an example, considering commercial building and Erzincan time history (figure 10), for PGA equal to 0.20g all the end sections of beams of 1st, 2nd and 3rd floors and the columns' base sections already reached chord rotation at yielding, while ultimate rotation was obtained for levels of seismic action generally higher than 0.35g. In any case, as visible from figures 10-12, beams and columns of the 5th floor were generally not involved in the development of ductile mechanisms for levels of seismic action lower than 0.50g. Similar considerations can be executed also for the other representative buildings analyzed.

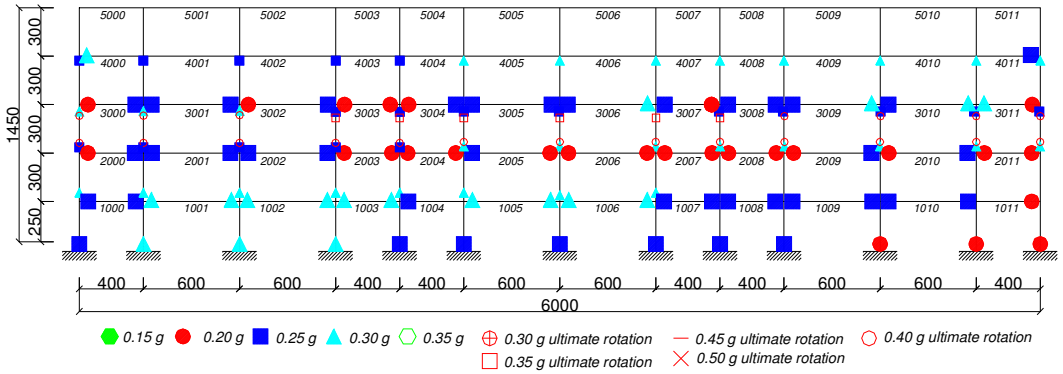

Figure 10: Structural behaviour of residential building in HDC for Erzincan earthquake.

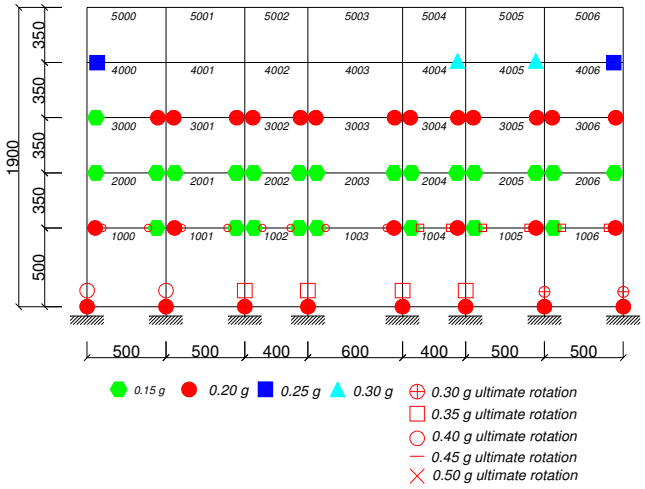

Figure 11: Structural behaviour of commercial building in HDC for Erzincan earthquake.

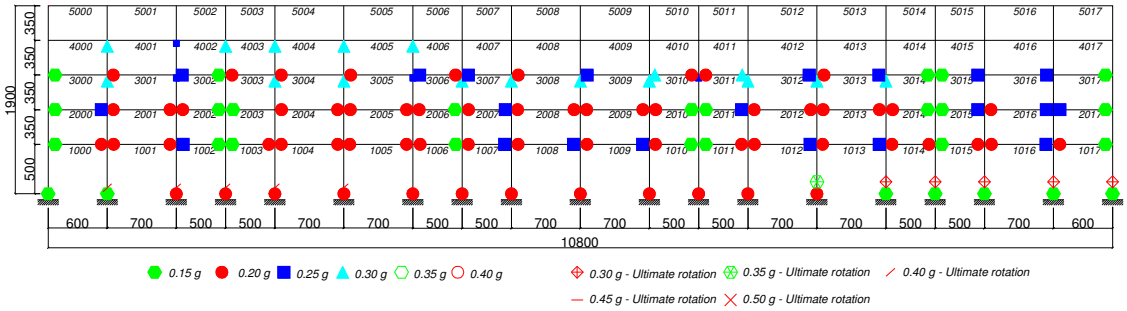

Figure 12: Structural behaviour of office building in HDC for Montenegro earthquake.

Looking at the structural behaviour of the residential building designed for LDC, some additional consideration shall be executed; as visible from figure 13, differently from what observed from buildings in HDC, some brittle mechanisms activated for levels of PGA between 0.25 and 0.30g, i.e. equal or slightly higher than the ones adopted in the design, in correspondence of the columns' base section of the 1st floor and, in some cases, at the ends of beams of the first storey. For what concerns, on the other hand, the ductile behaviour of structural elements, considerations similar to the ones presented for HDC buildings can be executed (figure 14), with first plastic hinges in correspondence of beams and columns of the first floors for PGA equal to 0.15g and the absence of ductile mechanisms at the 5th floor (beams and columns).

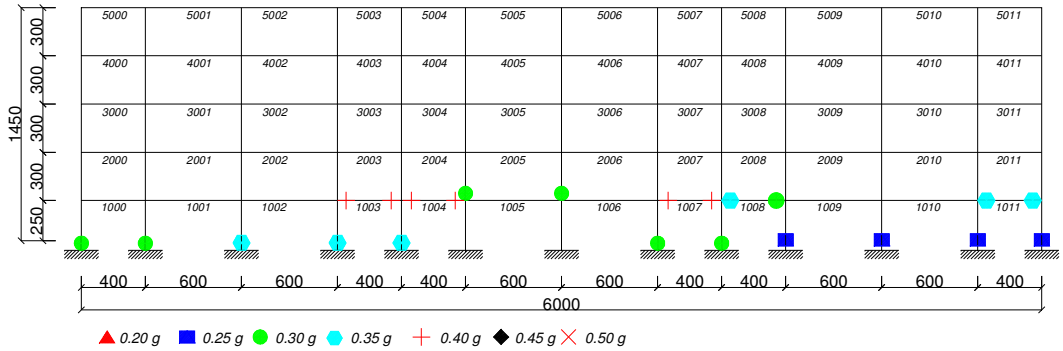

Figure 13: Structural behaviour of residential building in LDC for Erzincan earthquake: brittle mechanisms.

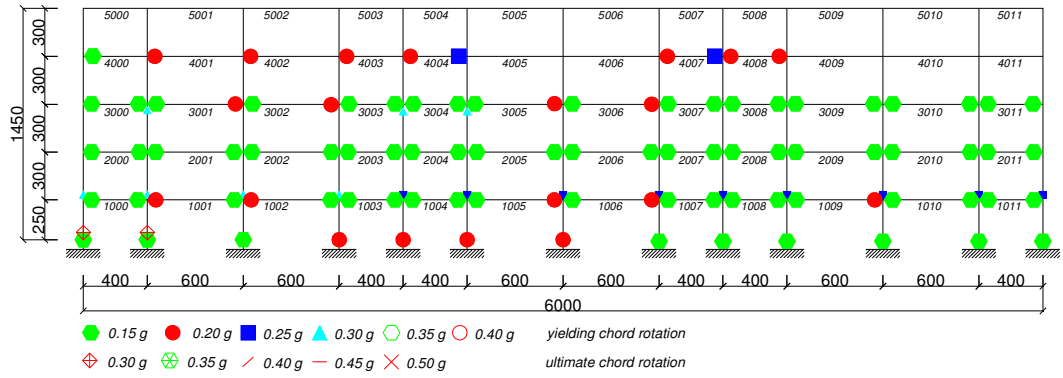

Figure 14: Structural behaviour of residential building in LDC for Campano Lucano earthquake: ductile mechanisms.

6 EVALUATION OF DUCTILITY DEMAND ON STEEL REINFORCING BARS

According to the formulation of the hardening slip model adopted for steel reinforcements, the results of IDAs on r.c. case studies are affected by the plastic hinge length: this means that while slips and stresses can be directly derived, further investigations are required for the effective strain levels on reinforcing bars. A simplified model of the bar was then elaborated and subjected to the stress histories coming from IDAs.

A zero-lenght element model [23] with Menegotto-Pinto law was used for the representation of the hysteretic behaviour of steel reinforcements, calibrating the parameters used for Steel02 material on the base of experimental LCF tests on steel reinforcing bars B450C presented in [27]. The calibration procedure was based on the first cycle tension-compression, since buckling generally happened after the first stress reversal and degradation phenomena were not taken into account.

Mean values of the mechanical properties (yielding strength R_e, tensile strength R_m, elongation to maximum load A_{gt}) of the corresponding steel grades, coming from the experimental mechanical tensile tests presented in [25], were adopted, while the hardening branch slope was defined according to Eqn. (8), in which ε_p represents the strain corresponding to the end of the yielding plateau (≅ 2.0%):

$$E_h = \frac{R_m - R_e}{A_{gt} - \varepsilon_p} \tag{8}$$

Finally, the parameters assumed for the Menegotto-Pinto law were the ones generally suggested by Mazzoni et al. [23]: $R0 = 0.20$, $cR1 = 0.925$, $cR2 = 0.15$.

6.1 Evaluation of the seismic ductility demand (D) on steel bars

A peak ground acceleration (PGA) equal to 0.25g, i.e. the design PGA for LS limit state according to the design codes used in the design [1, 2], was considered. In agreement to what already presented about the global structural behaviour of the buildings, steel reinforcing bars of 1st floor columns' base sections and of 1st and 2nd floors' beams were usually taken into consideration. The most significant results obtained are presented for each designed building.

Steel bars are individuated with an identification code (ID) providing the number of the element, according to the schematization adopted in figure 15, the section (i.e. s1 is the starting section and s6 the end section, figure 16) and the corresponding position of the bar (i.e. J or K, respectively on the top or on the bottom of the transversal plane section, figure 16).

Results are presented in terms of maximum and minimum deformation and stress and total density of dissipated energy, evaluated as presented by Apostolopoulos [20]:

$$W = \int \sigma \, d\varepsilon \tag{9}$$

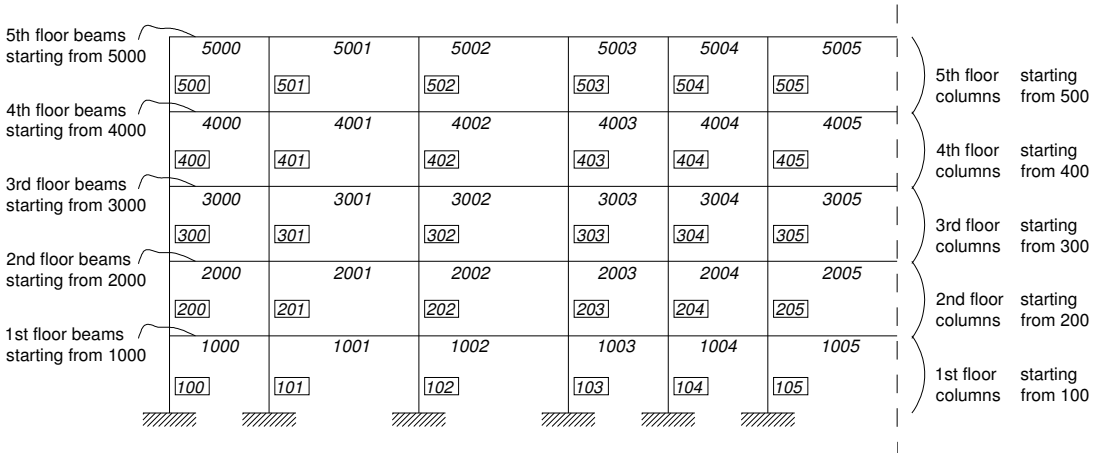

Figure 15: Schematization assumed for the identification of structural elements in the plane frames.

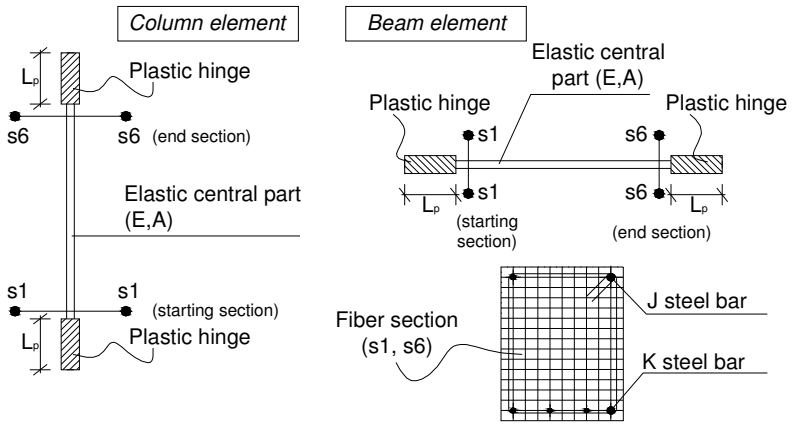

Figure 16: Schematization of section and steel fibre.

6.1.1 Residential building in HDC

The worst results in terms of maximum deformation level and dissipated energy were obtained considering Erzincan time history (figure 17); in the case of column n°112 (1st floor, external column) a maximum strain in tension equal to 5.45% was reached (steel bar S1K), while the minimum deformation in compression was equal to -3.26%. Despite the higher absolute values of strain, steel bars generally did not invert completely the sign of deformation, resulting in lower levels of dissipated energy (around 27 MPa). Similar considerations can be executed also for steel reinforcing bars in beam elements (table 7), in which the highest level of strain was equal to 5.03% (beam 1011, steel bar S6J) with dissipated energy density equal to 25 MPa.

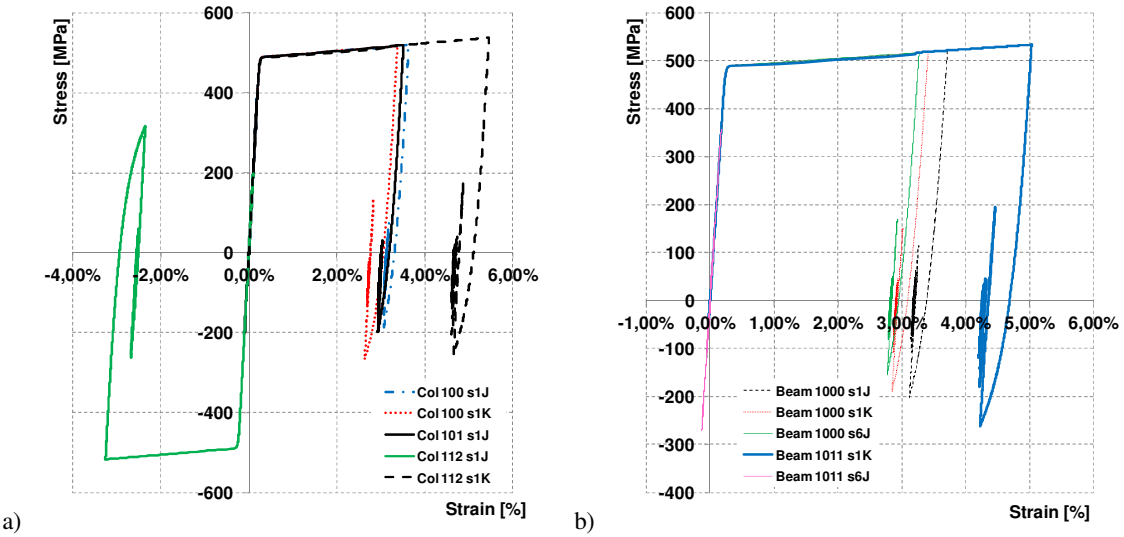

a) b)

Figure 17: Residential building in HDC, Stress-strain histories on steel bars for Erzincan time history: a) columns 1st floor, b) beams 1st level.

Residential building in HDC – Erzincan time history - COLUMNS						
Element ID	PGA 0,25g	Max. def. [%]	Min. def. [%]	Max. Tens. [MPa]	Min. Tens. [MPa]	Energy [MPa]
100	s1 J	3,63%	-0,05%	521,13	-193,24	17,11
	s1 K	3,37%	-0,06%	518,74	-266,61	16,11
101	s1 J	3,51%	-0,10%	520,02	-200,33	16,49
	s1 K	2,76%	-0,05%	513,08	-242,09	12,79
112	s1 J	0,10%	-3,26%	316,36	-517,67	16,00
	s1 K	5,45%	-0,02%	537,79	-254,33	27,08

Table 6: Stress and strain values on steel reinforcing bars of columns (residential building in HDC).

Residential building in HDC – Erzincan time history - BEAMS						
Element ID	PGA 0,25g	max def [%]	min def [%]	max Tens [MPa]	min Tens [MPa]	Energy [MPa]
1000	s1 J	3,72%	-0,05%	521,88	-201,11	17,55
	s1 K	3,41%	-0,03%	519,09	-189,63	15,98
	s6 J	3,27%	-0,03%	517,81	-153,94	15,19
	s6 K	3,52%	-0,06%	520,09	-179,71	16,50
1011	s1 J	0,16%	-0,11%	334,62	-227,15	0,00
	s1 K	4,69%	-0,02%	530,84	-255,81	23,02
	s6 J	5,03%	-0,02%	533,96	-261,45	24,87
	s6 K	0,17%	-0,13%	357,39	-271,17	0,00

Table 7: Stress and strain values on steel reinforcing bars of beams (residential building in HDC).

6.1.2 Commercial building in HDC

The ID codes adopted for structural elements of commercial building in HDC followed the indications presented in figure 15. Also in this case, the worst results in terms of maximum deformation level and dissipated energy were obtained for Erzincan accelerogram (figure 18); in the case of column n°107 (1st floor, external column) a maximum strain in tension equal to 7.42% was reached (steel bar S1K), while the minimum deformation in compression was equal to -4.00% (steel bar S1J), with corresponding deformation in tension up to 5.08% and dissipated energy density equal to 74.4 MPa. The maximum values of dissipated energy density were obtained in correspondence of column n°101 (steel bar S1J, with 121.83 MPa, table 8) and of beam n°1002 (steel bar s6K, with 120.85 MPa, table 9), in which the internal forces were able to completely invert the sign of strain and to complete tension/compression cycles (figure 18).

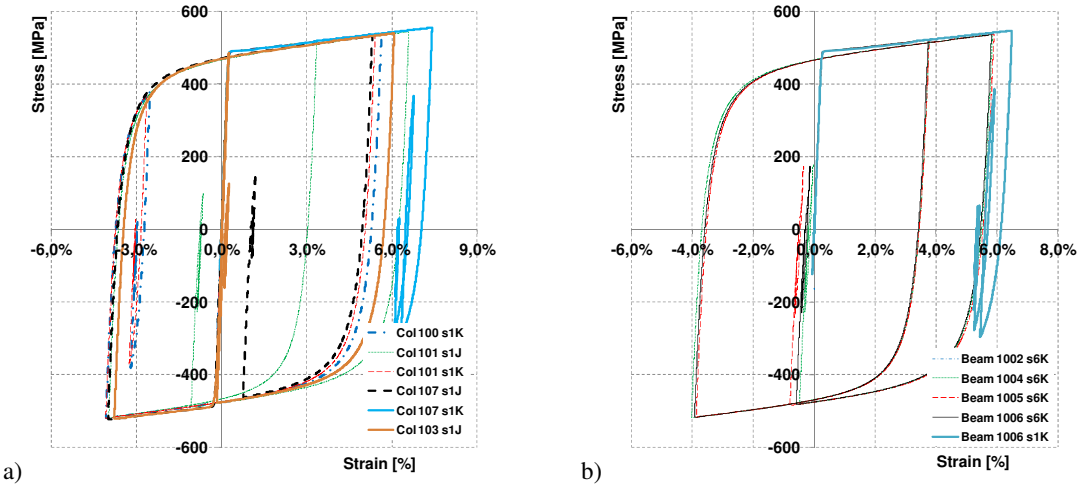

a) b)

Figure 18: Stress-strain histories on steel bars for Erzincan time history: a) columns 1st floor, b) beams 1st level.

Commercial building in HDC – Erzincan time history - COLUMNS						
Element ID	PGA 0,25g	max def [%]	min def [%]	max Tens [MPa]	min Tens [MPa]	Energy [MPa]
101	s1 J	6,60%	-3,97%	544,05	-518,95	121,83
	s1 K	5,41%	-4,08%	537,39	-520,64	68,98
103	s1 J	6,08%	-3,78%	540,04	-522,47	84,11
	s1 K	5,81%	-3,81%	541,04	-518,07	71,37
107	s1 J	5,31%	-4,00%	532,49	-524,49	74,37
	s1 K	7,42%	-0,05%	555,80	-294,51	39,17

Table 8: Stress and strain values on steel reinforcing bars of columns (commercial building in HDC).

Commercial building in HDC – Erzincan time history - BEAMS						
Element ID	PGA 0,25g	max def [%]	min def [%]	max Tens [MPa]	min Tens [MPa]	Energy [MPa]
1002	s1 J	5,46%	-0,011%	534,89	-351,68	32,14
	s1 K	5,83%	-0,081%	541,30	-470,25	50,49
	s6 J	5,46%	-0,057%	537,91	-312,72	28,60
	s6 K	6,08%	-3,852%	538,78	-517,80	120,85
1004	s1 J	5,40%	-0,012%	533,46	-387,31	33,09
	s1 K	6,09%	-0,072%	543,68	-399,72	37,16
	s6 J	5,58%	-0,050%	539,00	-292,56	28,83

1006	s6 K	5,85%	-4,030%	536,59	-519,60	116,42
	s1 J	4,88%	-0,013%	530,86	-352,06	28,16
	s1 K	6,49%	-0,060%	547,34	-297,64	34,16
	s6 J	5,95%	-0,041%	542,38	-283,86	30,63
	s6 K	5,82%	-3,930%	536,23	-518,56	115,44

Table 9: Stress and strain values on steel reinforcing bars of beams (commercial building in HDC).

6.1.3 Office building in HDC

The ID codes adopted for structural elements of commercial building in HDC followed the indications presented in figure 15. The results in terms of maximum deformation level and dissipated energy obtained for Montenegro time history are presented in the figure 19; in the case of column n°118 (1st floor, external column) a maximum strain in tension equal to 8.82% was reached (steel bar S1K), while the minimum deformation in compression was equal to -4.54% (column n°117 steel bar S1J). The maximum value of dissipated energy density was obtained in correspondence of column n°104 (steel bar S1J) with 101.18 MPa (table 10) and maximum and minimum strain respectively equal to 5.08% and -3.86%, in which the internal forces were able to completely invert the sign of deformation and to complete tension/compression cycles (figure 19). Similar considerations and values were obtained also for beam elements (figure 19b, table 11)

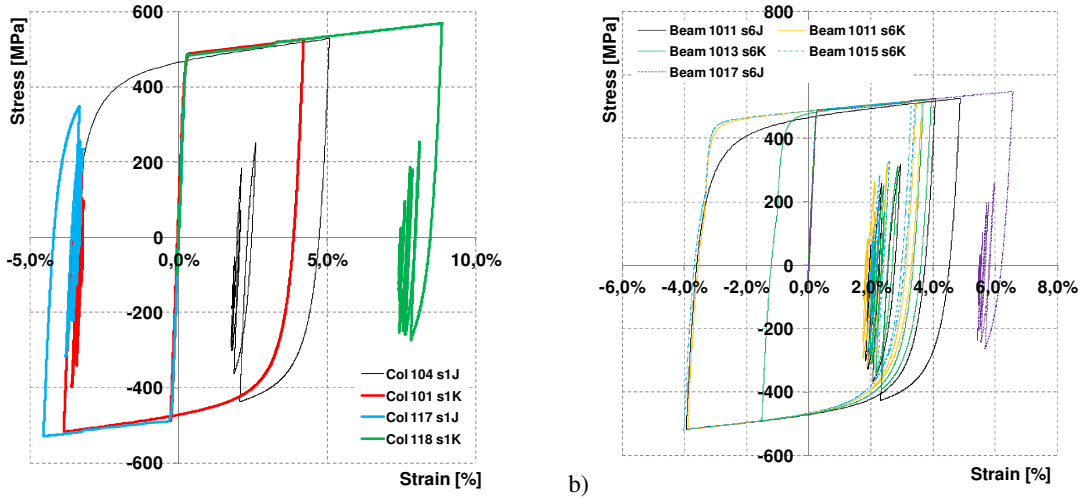

Figure 19: Stress-strain histories on bars for Montenegro time history: a) columns 1st floor, b) beams 1st level.

Office building in HDC – Montenegro time history - COLUMNS						
Element ID	PGA 0,25g	max def [%]	min def [%]	max Tens [MPa]	min Tens [MPa]	Energy [MPa]
104	s1 J	5,08%	-3,86%	528,63	-517,93	101,18
	s1 K	4,90%	-0,19%	532,70	-416,94	29,97
117	s1 J	0,17%	-4,54%	349,51	-529,48	24,14
	s1 K	7,92%	-0,09%	560,38	-274,88	41,38
118	s1 J	2,41%	-4,03%	502,49	-524,79	45,70
	s1 K	8,86%	-0,05%	569,05	-271,37	46,90

Table 10: Stress and strain values on steel reinforcing bars of columns (office building in HDC).

Office building in HDC – Montenegro time history - BEAMS						
Element ID	PGA 0,25g	max def [%]	min def [%]	max Tens [MPa]	min Tens [MPa]	Energy [MPa]
1011	s1 J	4,87%	-3,94%	526,63	-518,75	99,31
	s1 K	5,79%	-0,07%	540,86	-266,63	29,45
	s6 J	4,93%	-0,07%	532,98	-259,83	24,60
	s6 K	3,64%	-3,89%	520,78	-518,12	83,49
1015	s1 J	4,68%	-4,02%	524,76	-519,50	95,24
	s1 K	6,15%	-0,05%	544,21	-264,80	31,40
	s6 J	5,24%	-0,05%	535,82	-258,50	26,25
	s6 K	3,42%	-4,02%	518,95	-519,41	80,48
1017	s1 J	0,19%	-0,17%	388,01	-352,46	0,00
	s1 K	6,02%	-0,05%	543,02	-265,13	30,83
	s6 J	6,57%	-0,04%	548,02	-263,71	33,62
	s6 K	4,74%	-3,89%	525,28	-518,18	95,73

Table 11: Stress and strain values on steel reinforcing bars of beams (office building in HDC).

6.1.4 Residential building in LDC

Figure 15 shows the ID codes adopted for structural elements of residential buildings both in HDC and in LDC. The results in terms of maximum deformation level and dissipated energy obtained for Erzincan time history (figure 20); in the case of column n°111 (1st floor, external column) a maximum strain in tension equal to 4.84% was reached (steel bar S1K), while the minimum deformation in compression was equal to -5.18% (column n°111 steel bar S1J). The maximum value of dissipated energy density was obtained in correspondence of beam n°1011 (steel bar S6K) with 50.31 MPa (table 12) and maximum and minimum strain respectively equal to 4.82% and -3.24%, in which the internal forces were able to completely invert the sign of deformation and to complete tension/compression cycles (figure 20). The absolute maximum level of deformation, equal to 6.96%, was reached in correspondence of steel bar S1K in beam n°1010 (table 13).

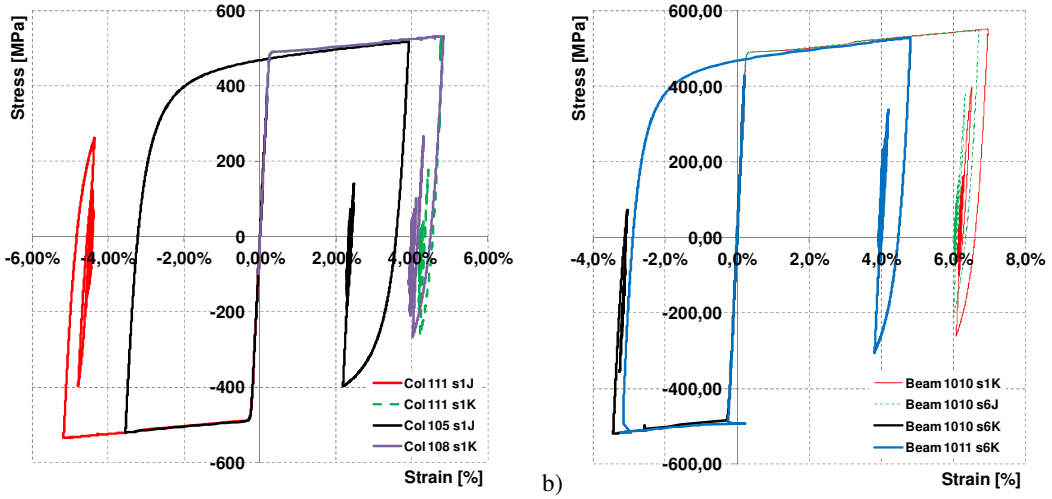

Figure 20: Stress-strain histories on bars for Erzincan time history: a) columns 1st floor, b) beams 1st level.

Residential building in LDC – Erzincan time history - COLUMNS						
Element ID	PGA 0,25g	max def [%]	min def [%]	max Tens [MPa]	min Tens [MPa]	Energy [MPa]
109	s1 J	0,15%	-5,06%	413,78	-534,25	30,66
	s1 K	4,08%	-0,04%	525,24	-263,35	19,65
105	s1 J	3,92%	-3,54%	518,41	-520,31	51,06
	s1 K	3,92%	-0,06%	523,80	-279,76	19,26
111	s1 J	0,13%	-5,18%	261,19	-535,26	25,88
	s1 K	4,84%	-0,04%	532,24	-262,58	23,65

Table 12: Stress and strain values on steel reinforcing bars of columns (residential building in LDC).

Residential building in LDC – Erzincan time history - BEAMS						
Element ID	PGA 0,25g	max def [%]	min def [%]	max Tens [MPa]	min Tens [MPa]	Energy [MPa]
1010	s1 J	0,14%	-0,15%	283,58	-312,18	0,00
	s1 K	6,96%	-0,04%	551,64	-260,57	35,53
	s6 J	6,71%	-0,03%	549,36	-210,40	33,68
	s6 K	0,20%	-3,44%	414,56	-519,36	15,71
1011	s1 J	3,63%	-0,16%	521,09	-321,58	16,95
	s1 K	5,63%	-0,03%	539,39	-280,50	27,91
	s6 J	5,44%	-0,02%	537,73	-271,56	26,20
	s6 K	4,82%	-3,24%	528,38	-517,50	50,31

Table 13: Stress and strain values on steel reinforcing bars of beams (residential building in LDC).

7 EVALUATION OF THE MECHANICAL CAPACITY OF STEEL BARS

7.1 Selection of the specimens

A representative set of steel reinforcing bars was selected inside the research project *Rusteel* in order to fully characterize the mechanical behaviour of the most significant steel grades actually used in Europe. All the most diffused mechanical production processes - TempCore (TEMP), Micro-Alloyed (MA), Stretched (STR) and Cold-Worked (CW) were considered, as well as different diameters (between 8 and 25 mm) and different producers (coming from France, Germany, Italy and Spain), in order to take into account the variability related to all the above mentioned aspects. Moreover, different steel grades (yielding strenght equal to 400, 450 or 500 MPa) and different ductility classes (A, B or C in relation to [21]) were selected. Table 14 presents the complete set of steel bars selected for experimental tests.

Steel Grade	Diameter	Steel Process	Ribs	Furniture	More information
B500A	8*,12*	CW	ribbed	Prod.1	
B500A	8*	CW	indented	Prod.2	
B500B	8*,16*,20*,25	TEMP	ribbed	Prod.1	Same cast for all diameters
	16*			Prod.2	From 3 different plants
B500B	8*,12	STR	ribbed	Prod.2	German plants
B400C	8*,16*,20*,25	TEMP	ribbed	Prod.2	Spanish plants
B400C	16*,20*,25	MA	ribbed	Prod.1	Same cast for all diameters
B450C	16*,20*,25	TEMP	ribbed	Prod.1	Same cast for all diameters
	16			Prod.2	From 3 different plants
B450C	8*,12*	STR	ribbed	Prod. 1+2	

Table 14: Selected steel grades for the mechanical characterization.

7.2 Execution of tensile and LCF tests on uncorroded specimens and results

Experimental tensile and low-cycle fatigue tests were executed on the bars presented in table 14; monotonic tensile tests were executed considering the prescriptions imposed by [35], while for the LCF tests an opportune protocol was elaborated inside Rusteel project, taking into consideration what provided by actual European standards [15, 16] and what presented in the current literature [19, 18].

The LCF protocol used for the experimental tests, briefly summarized in the table 15 for different diameters, prescribed the execution of symmetrical tension/compression cycles up to the failure of the bar with two different levels of imposed deformation, respectively equal to ±2.5% and ±4.0%, and two different free length of the specimens, respectively equal to 6ϕ and 8ϕ, corresponding to the minimum stirrups' spacing for buildings designed in HDC and LDC. The frequency to be used in the experimental tests was fixed equal to 2.0 Hz, but, according to what presented in Caprili [27], for high diameters (≥16mm) it was reduced to 0.5 Hz, since not significant differences in terms of dissipated energy were revealed.

Diameter ϕ [mm]	Frequency [Hz]	Free length L_0		Imposed strain ε [%]	Elongation Δl [mm]
20	0.05	6ϕ	120	± 2.5%	3.00
				± 4.0%	4.80
		8ϕ	160	± 2.5%	4.00
				± 4.0%	6.40
16	2.00	6ϕ	96	± 2.5%	2.40
				± 4.0%	3.84
		8ϕ	128	± 2.5%	3.20
				± 4.0%	5.12
12	2.00	6ϕ	72	± 2.5%	1.80
				± 4.0%	2.88
12	2.00	8ϕ	96	± 2.5%	2.40
				± 4.0%	3.84
8	2.00	6ϕ	48	± 2.5%	1.20
				± 4.0%	1.92
		8ϕ	64	± 2.5%	1.60
				± 4.0%	2.56

Table 15: Protocol for the execution of low-cycle fatigue tests on bars of different diameter.

Low-cycle fatigue tests results were analyzed in terms of maximum and minimum effective strain obtained (evaluated considering the contribution due to the machine deformability), maximum and minimum stress and density of dissipated energy, total and per cycle. In particular, in the present work the results obtained for steel reinforcing bars of diameter 16 mm, steel grade B450C and different producers are presented, in order to be compared with bars used in the design of representative r.c. buildings.

In the figures 21 and 22 the stress-strain diagrams obtained from bars B450C, diameter 16 mm, TempCore process are presented for the two different considered free lengths and imposed deformations. Moreover, figure 23 presents the trend of the dissipated energy density per cycle evaluated considering L_0=6ϕ and L_0=8ϕ. Table 17 presents the values of the effective maximum and minimum strain and stress on specimens and the total energy dissipated for all the considered specimens tested.

The behaviour of steel reinforcing bars of diameter 16 mm was more stable under lower level of imposed deformation, while for imposed strain equal to ±4.0%, despite higher values

of the dissipated energy density per cycle, the number of cycles up to failure rapidly decreased, showing, moreover, a more brittle behaviour in the case of free length equal to 8 diameters (figure 23). As an example, for $L_0=6\phi$ and imposed deformation equal to ±2.5%, steel bars B450C, diameter 16 (producer 1.1) were able to complete 19 cycles before failure without showing a significant decrease of the dissipative capacity per cycle; otherwise, considering a free length $L_0=8\phi$, the number of cycles before failure dropped to 9 with a sudden decrease of the dissipated energy per cycle. The total energy dissipated passed from 560 MPa to 260 MPa.

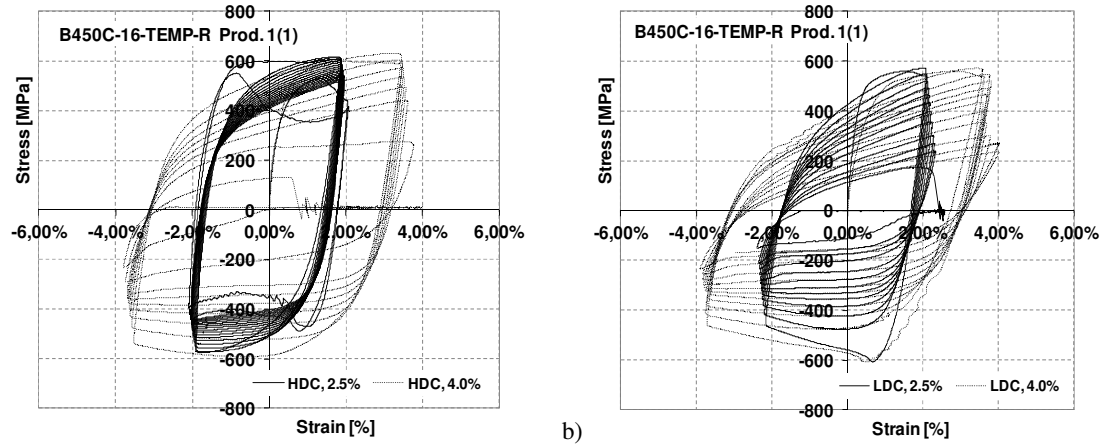

Figure 21: LCF tests on steel bars B450C-16-TEMP-R (Producer 1.1) for free length of the specimen equal to a) 6ϕ and b) 8ϕ and imposed deformation equal to ±2.5% and ±4.0%.

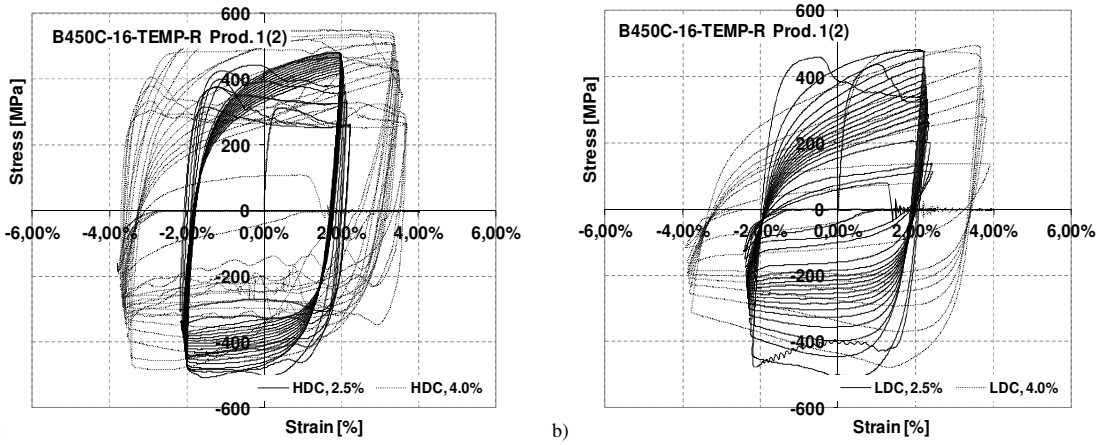

Figure 22: LCF tests on steel bars B450C-16-TEMP-R (Producer 1.2) for free length of the specimen equal to a) 6ϕ and b) 8ϕ and imposed deformation equal to ±2.5% and ±4.0%.

Specimen [-]	ϕ [mm]	L_0 [mm]	f [Hz]	Max ε [%]	Min ε [%]	Max σ [MPa]	Min σ [MPa]	Total dissipated energy [MPa]
B450C-16-TEMP-R Prod. 1(1)								
1	16	96	2	2,07%	-2,10%	616,66	-575,38	558,67
2	16	96	2	4,01%	-3,77%	631,22	-591,83	378,13
3	16	128	2	2,58%	-2,39%	572,16	-607,34	261,50
4	16	128	2	4,02%	-3,91%	613,85	-540,82	471,51
B450C-16-TEMP-R Prod. 1(2)								
1	16	96	2	2,23%	-2,18%	483,44	-508,73	516,86
2	16	96	2	4,01%	-3,80%	550,74	-483,86	726,01
3	16	128	2	2,51%	-2,43%	482,54	-508,39	353,75
4	16	128	2	4,01%	-3,93%	494,73	-477,06	230,29
B450C-16-TEMP-R Prod. 1.3								
1	16	96	2	2,19%	-2,10%	537,65	-557,82	532,15
2	16	96	2	4,03%	-3,76%	465,48	-515,36	550,99
3	16	128	2	2,51%	-2,37%	501,91	-550,97	291,96
4	16	128	2	4,50%	-3,92%	598,09	-491,88	380,03
B450C-16-TEMP-R Prod. 2								
1	16	96	2	2,51%	-2,26%	562,50	-560,12	477,75
2	16	96	2	2,51%	-2,41%	552,44	-555,05	329,95
3	16	128	2	4,10%	-3,81%	531,52	-502,24	316,67
4	16	128	2	4,11%	-3,92%	510,48	-471,70	224,46

Table 16: Maximum and minimum strain and deformation and total energy dissipated for B450C diameter 16 mm TempCore bars (producers 1.1, 1.2, 1.3 and 2).

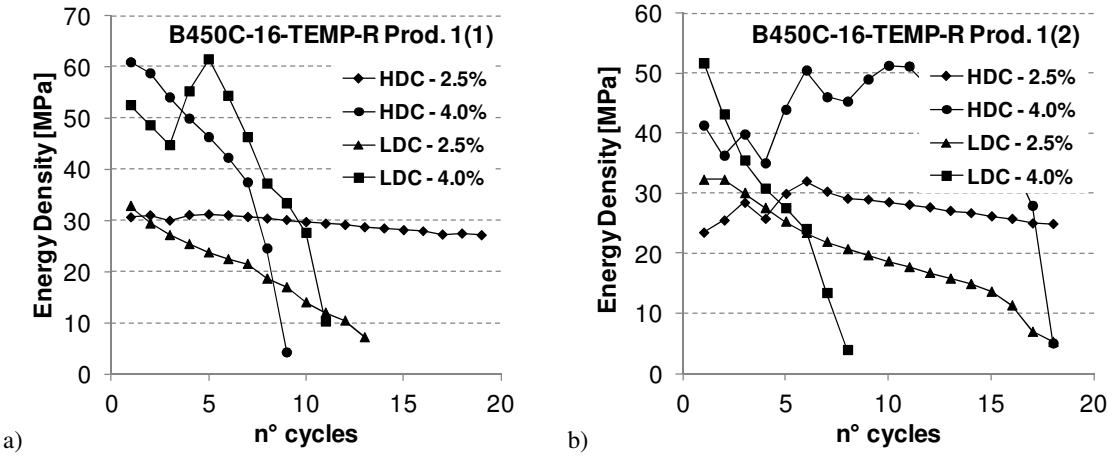

Figure 23: Dissipated energy density per cycle for bars B450C-16-TEMP: a) prod. 1.1, b) prod. 1.2.

All the LCF tests evidenced large buckling deformations of the specimens, independently from the test variables, i.e. type of bar and amplitude of the applied cycles. Buckling phenomena generally happened at the first cycle in compression, leading to values of the maximum strength at failure lower than the ones obtained from tensile tests. Moreover, the number of cycles up to failure generally decreased with the increase of the level of imposed deformation and of the free length of the specimen; as an example, for $L_0=6\phi$ and imposed strain equal to ±2.5% steel reinforcements were able to complete at least 18 cycles, independently from the diameter of the rebar and from the steel grade. The decrease of the

dissipated energy per cycle was, in general, quite uniform, even if some exceptions were individuated: as visible from figure 24, steel bars B450C (producer 2) exhibited a rapid decrease of dissipated energy after 15 cycles, differently from all the other considered specimens (different producer and plants).

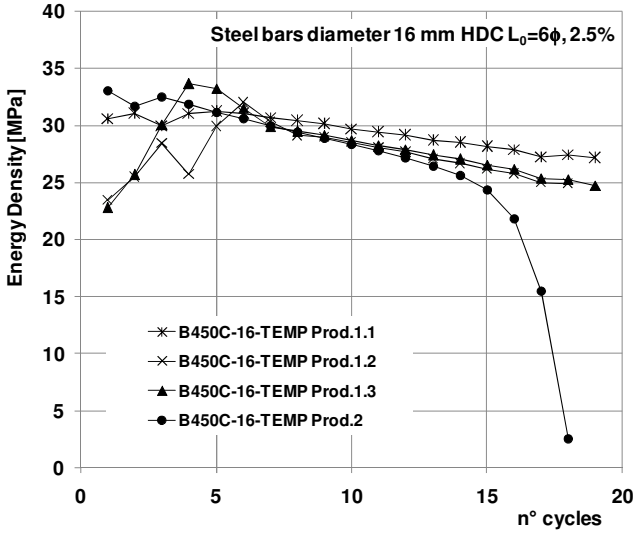

Figure 24: Dissipated energy per cycle for steel bars diameter 16 mm, $L_0 = 6\phi$ and ε equal to $\pm 2.5\%$.

7.3 Mechanical characterization of corroded steel bars

7.3.1 Elaboration of a protocol for accelerated corrosion tests

Recent studies in the current literature [20, 22] evidenced the progressive deterioration of the mechanical characteristics of steel reinforcing bars under aggressive environmental conditions. The effects of corrosion on the mechanical properties of bars were not usually taken into account since the presence of a correctly sized concrete cover, joined with ordinary external circumstances, is generally sufficient to guarantee the protection of reinforcing steel bars, providing a thin passive layer that covers the reinforcement avoiding the generation of rust. If the pH falls to values below 11 (in the case of degraded concrete the pH is close to 6.5), the passive layer starts to crack, becoming no more able to protect the spread of corrosion and leading to a decrease of the mechanical properties (strength and ductility) of bars. The effects of corrosion on steel reinforcing bars can be summarized in three main aspects:

- the reduction of the cross section of the bar (mass loss) with consequent decrease of the load carrying capacity, increasing with the duration of the exposure time;
- the cracking and spalling of concrete, leaving the reinforcements more exposed to buckling phenomena;
- the reduction of the ductility, expressed in terms of elongation to maximum load (A_{gt}).

In *Rusteel* project, a detailed investigation of the mechanical behaviour of corroded steel reinforcing bars was developed in order to individuate the effects of aggressive environmental conditions on both the tensile and the low-cycle fatigue mechanical properties.

A specific protocol for the execution of accelerated corrosion tests in salt-spray chamber was elaborated on the base of ISO 9227: the protocol foresees the execution of wet/dry cycles of 90 minutes (90 minutes dry, 90 minutes wet, resulting in 8 cycles/day) with a pH of the salt spray chamber between 5.5 and 6.2. Specimens of 500-600 mm length shall be opportunely prepared protecting them with a wax cover leaving free to corrode only a central part of about 20 mm (or the medium distance between subsequently ribs, Figure 25b-25c); the specimens

shall be positioned in salt spray chamber with a slope of 60° respect to the vertical walls of the chamber in order to prevent salt generation (figure 25a). After the end of the exposure period and before the execution of mechanical tests, steel corroded bars shall be maintained at a temperature lower than -5°, in order to kept inside the Hydrogen volatile part eventually developed during the salt-spray tests, that can lead to premature brittle failures of bars.

A reduced set of steel bars was selected to be subjected to corrosion for periods of 45 or 90 days of corrosion (table 17), and for the following execution of tensile and LCF tests. In the following, according to what already presented for uncorroded rebars, the results coming from steel reinforcements B450C, diameter 16 mm TempCore are presented.

ID	Quality	ϕ	Producer	Surface	Process	Salt-Spray chamber 45 days		Salt-Spray chamber 90 days	
-	-	-	-	-	-	N° Tensile tests	N° LCF tests	N° Tensile tests	N° LCF tests
1	B500B	16	2	Ribbed	TEMP	3	-	6	5*
2	B450C	16	2	Ribbed	TEMP	3	-	6	5*
3	B400C	16	2	Ribbed	TEMP	3	-	6	5*
4	B400C	16	1	Ribbed	MA	3	-	3*	5*
5	B500A	12	1	Ribbed	CW	3	-	3*	5*
6	B500B	25	1	Ribbed	TEMP	3	-	3*	5*
7	B500B	12	2	Ribbed	STR	-	-	3*	5*
8	B400C	25	1	Ribbed	MA	3	-	3*	5*
9	B450C	12	2	Ribbed	STR	-	-	3*	5*
10	B450C	25	1	Ribbed	TEMP	3	-	3*	5*

Table 17: Steel bars selected for salt-spray chamber tests and tests foreseen.

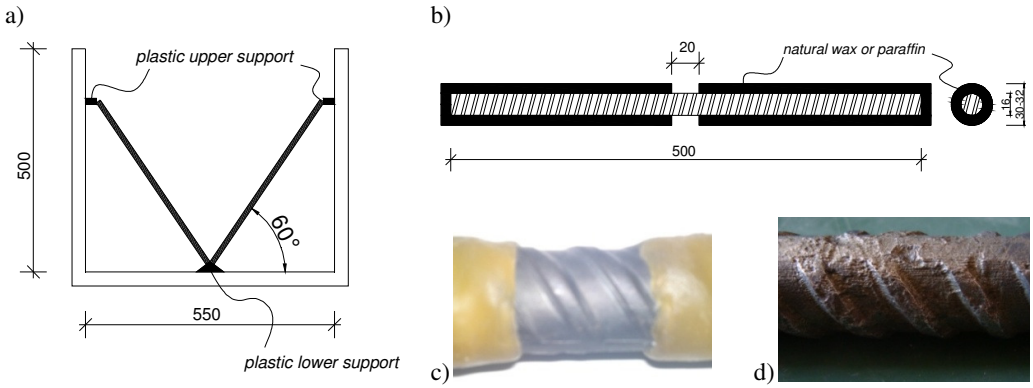

Figure 25: a) Disposition of bars in salt-spray chamber, b-c) protection of rebar with paraffin or wax, d) one specimen after 90 days in salt-spray chamber.

7.3.2 Results of tensile tests on corroded specimens

The results obtained from uncorroded and corroded specimens B450C diameter 16 mm (TempCore) after 45 and 90 days of exposure in salt spray chamber are presented and compared. Figure 26 shows the comparison between the stress-strain curves obtained from tensile tests on corroded and uncorroded specimens, while the values of yielding and tensile strength, A_{gt} and total elongation in corroded and uncorroded specimens are respectively presented in tables 18 and 19.

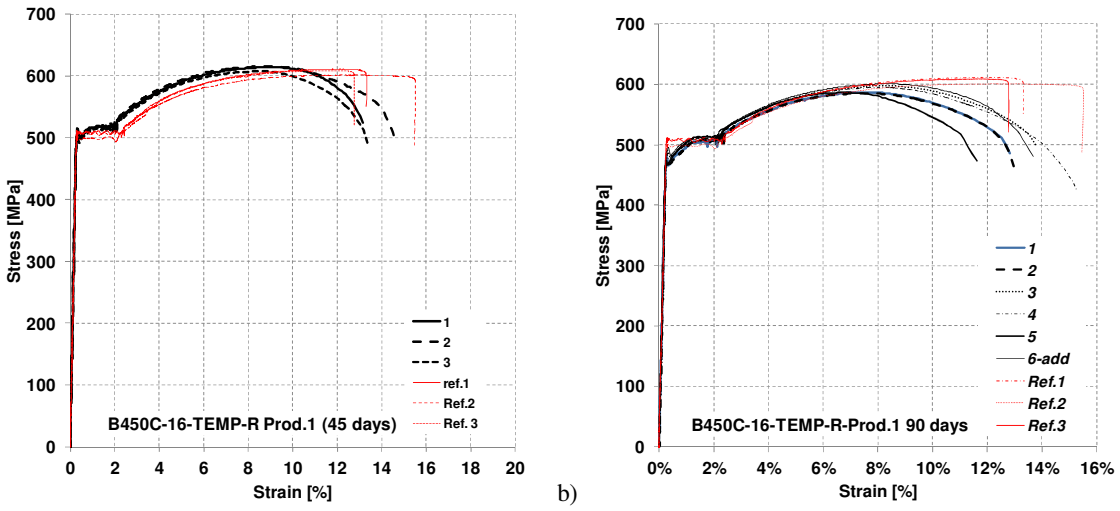

Figure 26: Stress-Strain diagrams for bars B450C-16-TEMP-R (prod. 1): a) 45 days of corrosion, b) 90 days.

Steel grade/diameter/ process/rib/producer	T_{corr} [days]	L_{corr} [mm]	ΔM [g]	$\Delta M/M_{uncorr}$ [%]	R_e [MPa]	R_m [MPa]	R_m/R_e [-]	A_{gt} [%]	A_5 [%]	Lab
B450C-16-TEMP-Prod.1-1	90	20,90	4,91	14,57	481,4	599,5	1,25	4,3	15,4	Lab. 1
B450C-16-TEMP-Prod.1-2	90	26,40	2,59	6,08	484,4	598,0	1,23	4,4	15,6	Lab. 1
B450C-16-TEMP-Prod.1-3	90	27,20	3,83	8,74	499,8	610,5	1,22	5,1	16,6	Lab. 1
B450C-16-TEMP-Prod.1-4	90	28,85	3,20	6,87	497,4	607,9	1,22	5,7	17,8	Lab. 1
B450C-16-TEMP-Prod.1-5	90	24,20	3,25	8,32	480,9	600,0	1,25	4,1	14,1	Lab. 1
B450C-16-TEMP-Prod.1-6	90	24,50	6,82	17,26	502,8	613,8	1,22	5,5	16,3	Lab. 1
B450C-16-TEMP-Prod.1-1	45	30,50	3,87	7,87	509,2	614,3	1,21	6,9	16,4	Lab. 1
B450C-16-TEMP-Prod.1-2	45	29,50	3,54	7,44	511,2	615,9	1,20	6,2	16,9	Lab. 1
B450C-16-TEMP-Prod.1-3	45	28,80	5,18	11,15	504,3	607,9	1,21	5,7	16,4	Lab. 1

Table 18: Experimental tensile tests on corroded specimens B450C TempCore, 16 mm (Prod. 1)

Steel grade/diameter/ process/rib/producer	Spec. [n°]	D [mm]	A [mm^2]	R_e [MPa]	R_m [MPa]	R_m/R_e [-]	A_{gt} [%]	A_5 [%]
B450C-16-TEMP-R Prod. 1	1	16,16	205,00	517,78	615,41	1,19	13,76	25,38
	2	16,18	205,71	507,42	610,42	1,20	14,96	25,13
	3	16,18	205,59	516,30	613,65	1,19	11,96	-

Table 19: Experimental tensile tests on uncorroded specimens B450C TempCore, 16 mm (Prod. 1)

As visible from table 18, results are presented in terms of mass loss, opportunely evaluated referring to the exposed length of the bar; the most significant results are the ones related to A_{gt}, that passed from a mean value of about 12% of uncorroded specimens, to values variable between 4.1% and 6.9% in relation to the exposure period (90 or 45 days). Deterioration of the mechanical characteristics in terms of yielding and tensile strength were also revealed, even if less significant.

7.3.3 Results of LCF tests on corroded specimens

Results of low-cycle fatigue tests executed on corroded specimens B450C, diameter 16 mm, TempCore process following the protocol previously presented are reported in the Figures 27 and 28 in terms of stress strain curves. In general three different specimens were tested for each level of imposed deformation and free length of the specimens, in order to

obtained significant data also in relation to different mass loss.

Moreover, table 20 shows the values of mass loss for each corroded specimen, the main testing specifications adopted and the total dissipated energy density obtained. In the figures 29 and 30 the dissipated energy per cycle is presented comparing the results obtained from corroded and uncorroded specimens, in all the different testing conditions considered. As visible, the behaviour of uncorroded specimens is more stable than the one associated to corroded bars: for example, in the case of $L_0=6\phi$ and ±2.5% of imposed strain, the total dissipated energy varied between 535 MPa (uncorroded specimen) and 370 MPa (corroded specimens), with a more sudden collapse in these last cases and number of cycles up to failure dropping from 19 to 15. Similar considerations can be executed also for $L_0=6\phi$ and ±4.0%, with total dissipated energy equal to 550 MPa for the uncorroded bars and around 300 MPa for corroded ones, with number of cycles up to failure dropping from 15 to 7.

Similar considerations can be executed also in the case of LDC ($L_0=8\phi$): for imposed strain equal to ±2.5% the total dissipated energy dropped from 290 MPa to 250 MPa (mean value), while for imposed strain equal to ±4.0% the difference was between 380 MPa and 250 MPa.

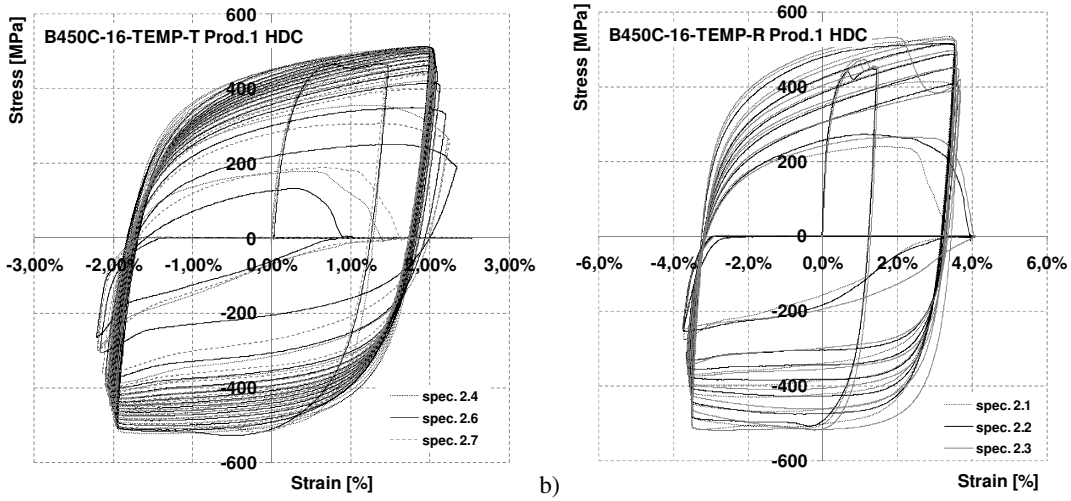

Figure 27: Steel bars B450C-16-TEMP-R (prod. 1) after 90 days and $L_0=6\phi$, for : a) $\varepsilon = \pm 2.5\%$ and b) $\varepsilon = \pm 4.0\%$.

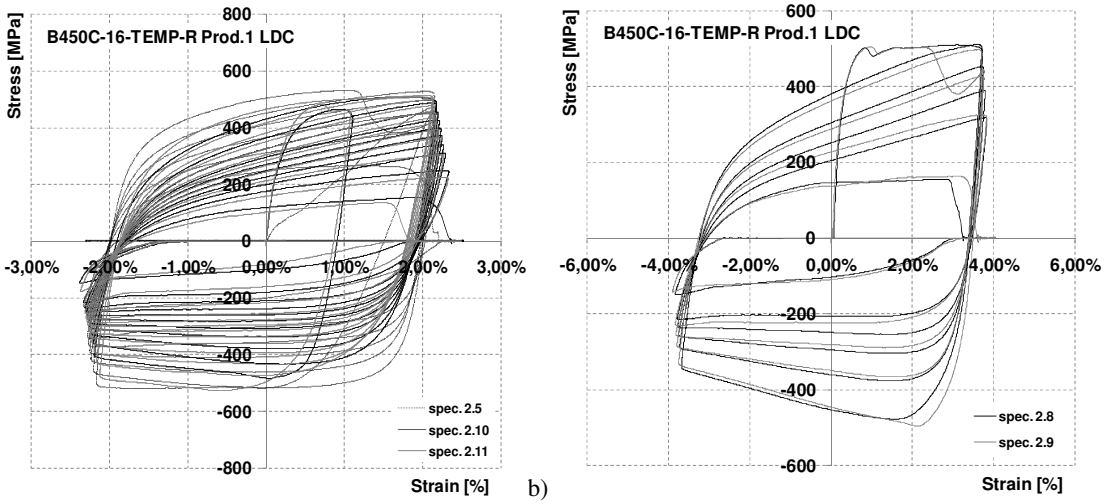

Figure 28: Steel bars B450C-16-TEMP-R (prod. 1) after 90 days and $L_0=8\phi$, for : a) $\varepsilon = \pm 2.5\%$ and b) $\varepsilon = \pm 4.0\%$.

B450C-16 -TEMP Prod. 1 90 days (Laboratory 2)									
ID	M_{uncorr} [g]	L [mm]	M_{corr} [g]	L_{corr} [mm]	ΔM [g]	$\Delta M/M_{uncorr}$ [%]	L_0 [mm]	$\Delta\varepsilon$ [%]	Dissipated Energy [MPa]
2.4	808,42	501,00	805,96	19,90	2,46	7,66%	96	±2.5%	371,28
2.6	805,92	500,00	802,48	22,65	3,44	9,43%	96	±2.5%	370,80
2.7	810,25	501,00	808,04	18,60	2,21	7,33%	96	±2.5%	377,30
2.1	809,35	500,00	806,75	20,75	2,60	7,74%	96	±4.0%	307,28
2.2	810,34	501,00	806,89	22,40	3,45	9,53%	96	±4.0%	291,32
2.3	806,88	500,00	804,18	21,15	2,70	7,91%	96	±4.0%	306,62
2.5	810,50	500,00	807,69	21,20	2,81	8,18%	128	±2.5%	213,59
2.10	808,78	501,00	804,68	27,10	4,10	9,36%	128	±2.5%	215,10
2.11	808,11	501,00	804,58	23,83	3,53	9,18%	128	±2.5%	273,49
2.8	806,38	500,00	803,71	23,90	2,67	6,92%	128	±4.0%	206,68
2.9	809,54	501,00	807,39	20,55	2,15	6,49%	128	±4.0%	172,60

Table 20: Characteristic of corroded steel reinforcing bars B450C, 16 mm, TempCore and testing specifications.

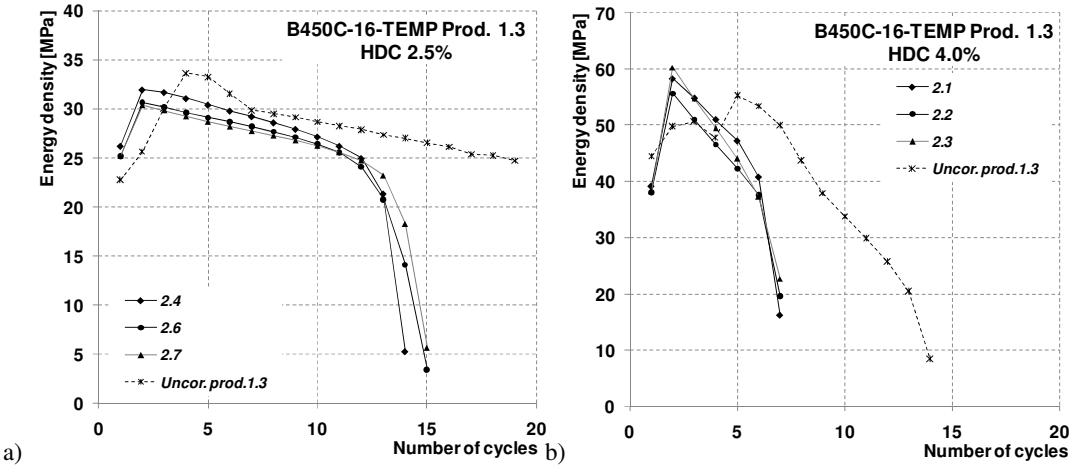

a) b)

Figure 29: Comparison between corroded and uncorroded specimens B450C, diameter 16 mm (TempCore) in terms of dissipated energy per cycle: a) HDC and imposed deformation ±2.5% and b) HDC and ±4.0%.

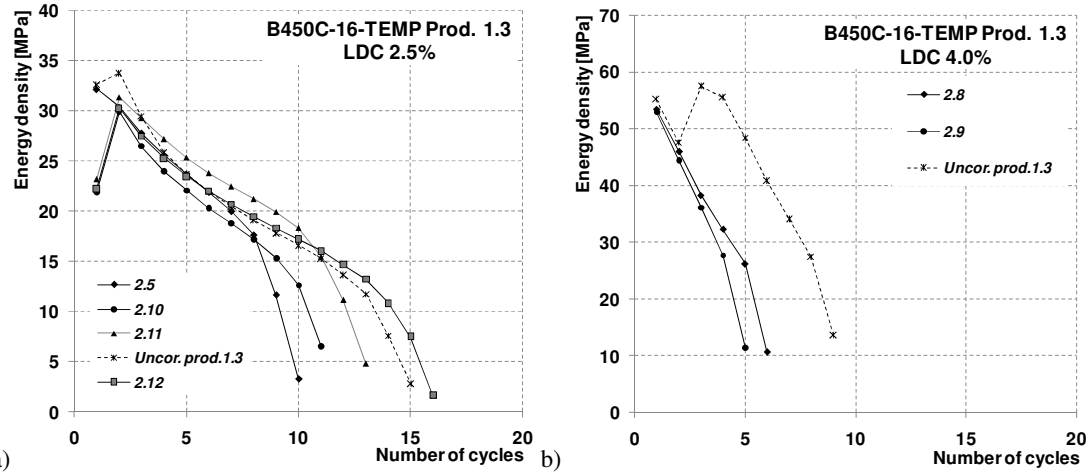

a) b)

Figure 30: Comparison between corroded and uncorroded specimens B450C, diameter 16 mm (TempCore) in terms of dissipated energy per cycle: a) LDC and imposed deformation ±2.5% and b) LDC and ±4.0%.

8 CONCLUSIONS

In the present paper a specific procedure for the evaluation of the effective ductility demand on steel reinforcing bars in modern r.c. buildings was presented and applied to a set of significant case studies. Moreover, a detailed experimental test campaign was executed aiming at the complete mechanical characterization of the monotonic and cyclic behaviour of actual European steel reinforcing bars, both in uncorroded and in corroded conditions.

The effective levels of deformations induced by seismic events on bars were evaluated through the execution of Incremental Dynamic Analyses on a set of representative r.c. buildings opportunely designed according to the actual European and Italian prescriptions [1, 2], using the hardening slip model [27, 28] for steel reinforcing bars embedded in the concrete, able to include relative slips between steel bars and concrete and to fully characterize their cyclic behaviour.

IDAs were executed on the bi-dimensional fiber models of r.c. case studies opportunely elaborated using OpenSees software; specific natural time histories, selected to maximize the seismic requirements in terms of both energy dissipation and deformation, were used. The global seismic assessment of buildings, following the indications of actual design standards, evidenced a different behaviour between buildings designed in HDC or LDC, with the activation of brittle shear mechanisms in beams and columns of the 1st floor for levels of p.g.a. more or less equal to the one adopted in the design in the case of LDC. Moreover, despite what imposed during the design process according to the capacity design approach, the global assessment of the structures evidenced that beams and columns of the highest floors of the buildings (4th and 5th levels) were usually not directly involved in the global collapse mechanisms, since in general plastic hinges developed for very high values of the PGA (higher than 0.40-0.45g).

The investigation of the local ductile behaviour of steel reinforcing bars allowed, moreover, the individuation of the effective levels of deformation and energy dissipation due to real seismic action. The accurate analysis of numerical simulations' results evidenced two main general stress-strain conditions in steel reinforcing bars, in relation to both the level of axial deformation and the dissipated energy density. The first condition, well evidenced in the Figure 34, was typical of those elements, generally beams but in some cases also columns, in which the level of imposed deformation due to earthquakes was usually very high, around 8%, while the corresponding density of dissipated energy generally did not overpass 40-50 MPa, since the external axial load generally did not generate complete reversed cycles of tension/compression stresses and strains, with following very low values of deformation in compression (not higher than -1%). As an example, figure 31 shows the stress-strain curves obtained from steel reinforcing bars in column n°118 and in beam n°1017 (figure 15) in office building under, respectively, Erzincan and Montenegro time histories; the maximum level of strain in tension was equal to 8.86% and 6.57% and the corresponding dissipated energy was equal to 33.6 MPa and 46.9 MPa.

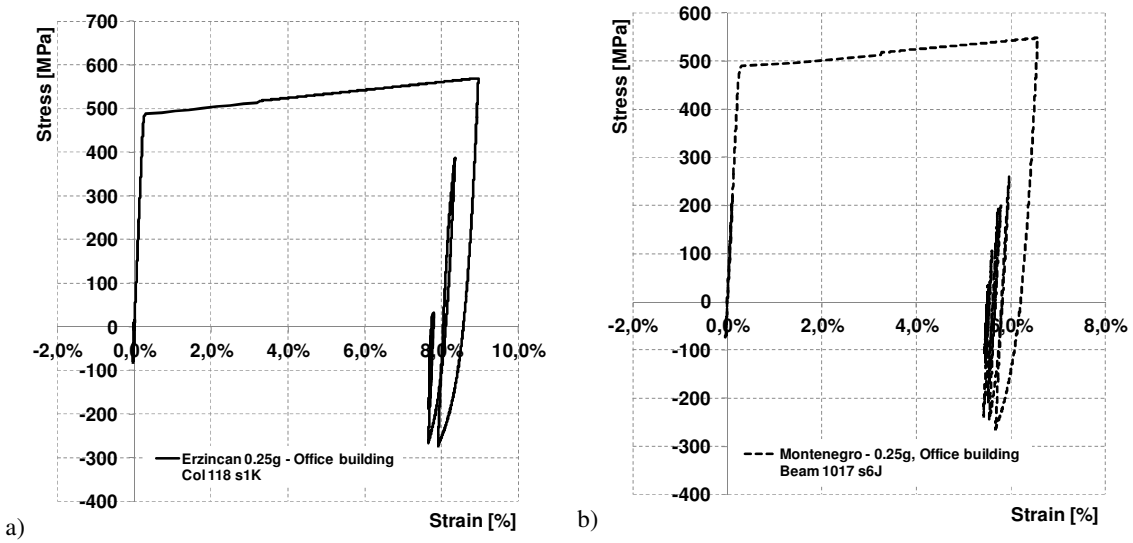

Figure 31: Stress-strain histories on bars characterized by mainly tension or compression.

The second condition, represented in the figure 32, at the opposite, was typical of those elements in which the seismic input was able to generate on steel reinforcing bars complete reversed tension/compression cycles; as a consequence, high absolute values of strain both in tension and in compression were reached (with mean values around 6% and -4%) and also the density of dissipated energy increased with respect to the other condition, with values up to 120 MPa. As an example, in the figure 32 the stress-strain curves obtained from steel reinforcing bars in columns n°101 and n°118 in office building under, respectively, Erzincan and Campano Lucano time histories; the maximum level of strain in tension was equal to 6.04% and 4.02% and the ones in compression were equal to -4.0%, while the corresponding dissipated energy generally varied between 90 and 120 MPa.

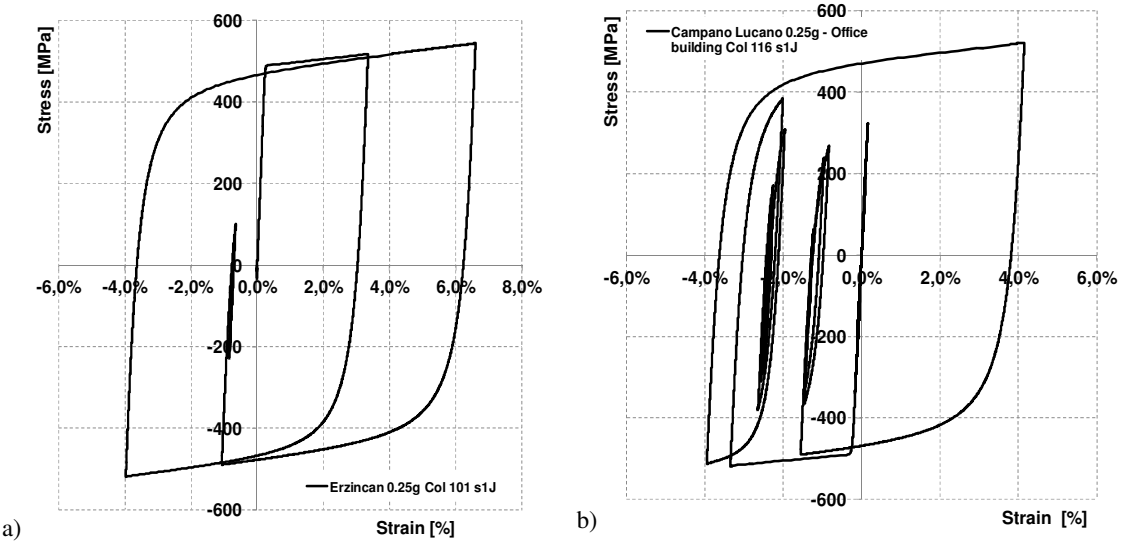

Figure 32: Stress-strain histories on bars subjected to complete reversed tension/compression cycles.

It's important to underline that, according to the numerical results obtained, natural time histories generated only one or two complete tension/compression cycles in steel reinforcing bars confirming, at the same time, the assumptions used for the calibration of the mechanical

model of the bar.

At the same time, for what concerns the evaluation of the mechanical capacity of steel reinforcing bars, experimental tensile and low-cycle fatigue tests were executed on a set of steel reinforcing bars representative of the actual European production. Tensile tests followed the prescriptions of EN 15630-1:2010 [35] while for LCF tests a new protocol was elaborated, taking into account what actually presented in literature and in the current standards (Spanish and Portuguese codes). Moreover, the effects of corrosion phenomena on the mechanical properties of steel reinforcing bars were evaluated: accelerated corrosion tests in salt spray chamber were executed on a reduced set of reinforcing steels considering two different exposure periods (45 and 90 days). Tensile and low-cycle fatigue were consequently executed on corroded specimens.

The results of tensile tests on corroded bars evidenced a strong reduction of the ductile capacity of steel bars, mainly in terms of A_{gt}, that for reinforcements B450C, diameter 16 mm (TempCore process) in some cases dropped from an initial mean value of 12% to values around 4-6%, for an average mass loss between 16 and 20%. Results similar to the ones obtained for B450C were individuated for all TempCore steel bars, while in general, Micro Alloyed steel showed a lower decrease of A_{gt} and higher reference values.

Looking at the low-cycle fatigue behaviour of corroded steel reinforcements, corroded steel reinforcing bars B450C diameter 16 mm evidenced a strong reduction of the total dissipated energy density with respect to the uncorroded condition, both considering a free length equal to six or eight diameters and for imposed deformation equal to ±2.5% or ±4.0%.

Despite the reduction of the dissipated energy density, comparing the results obtained from IDAs the maximum dissipated energy obtained in steel reinforcing bars of beams and columns of the designed r.c. buildings was equal to 121 MPa, and consequently also corroded rebars are able to satisfy the energy requirements due to seismic action. On the other hand, the worst problem consists in the strong reduction of the A_{gt}, reaching values lower than the maximum strain obtained from numerical simulations, in some cases around 8.0% (figure 33).

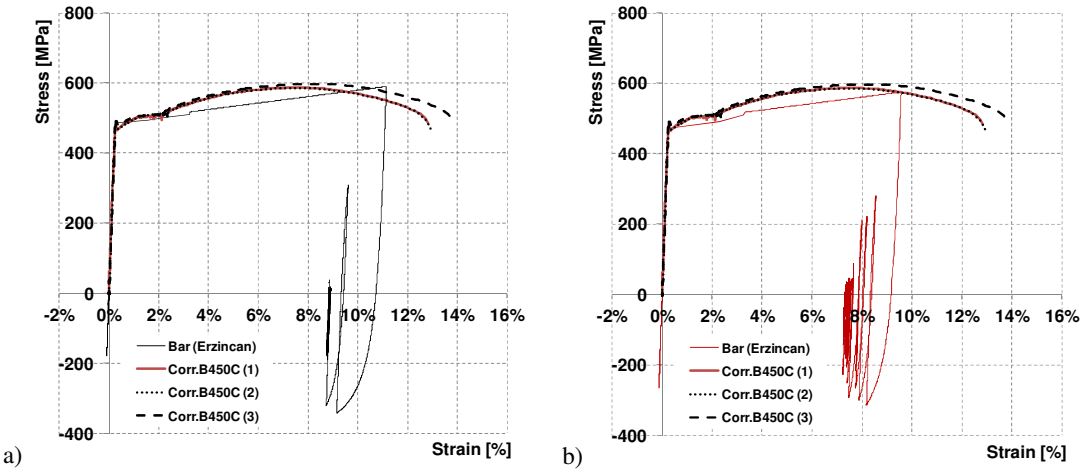

Figure 33: Comparison between the ductility demand imposed by Erzincan time history on a) 1st floor column's bar and b) beam's 1st floor bar and monotonic behaviour of corroded steel reinforcements (bar B450C, 16 mm).

As an example, the results of the Incremental Dynamic Analyses showed that the level of strain due to real seismic inputs in some cases reached maximum values around 8.8%, while usually, the 6-7% of deformation was overpassed. Moreover, in many cases, bars were subjected to a complete reversed tension/compression cycle with imposed strain equal, for example, to +6.30% - 4.25%. The behaviour of corroded bars (in this case steel grade B450C,

diameter 16 mm) is compared with the results of analysis for steel reinforcements in one column or in one beam of the first floor; the maximum strains imposed by seismic event were respectively equal to about 11% and 9%, while the average A_{gt} of corroded bars varied between 4.3% and 5.7% (manually measured values). Obviously, corroded bars also presented a residual deformation capacity, as presented in the figures 33, leading to values of the total elongation varying between 14% and 16%.

REFERENCES

[1] UNI EN 1998-1:2005, Eurocode 8 - Design of structures for earthquake resistance - Part 1: General rules, seismic actions and rules for buildings, 2005

[2] D. M. Infrastrutture Trasporti 14 gennaio 2008, Norme Tecniche per le Costruzioni NTC 2008.

[3] FEMA 356 (2000). Pre-standard and Commentary for the Seismic Rehabilitation of Buildings, Federal Emergency Management Agency, Washington DC.

[4] A. Teran-Gilmore, O. Jirsa, Energy demands for seismic design against low-cycle fatigue. *Earthquake engineering and structural dynamics,* **36**, 383-404, 2007.

[5] T. Paulay, M.J.N. Priestley, *Seismic design of reinforced concrete and masonry structures*, John Wiley and Sons, 1992.

[6] S.K. Kunnath, Q. Hu, Evaluation of cyclic demand in ductile RC structures. *13th World Conference on Earthquake Engineering*, Vancouver, Canada, August 1-6, 2004.

[7] G. Manfredi, M. Polese, E. Cosenza, Cumulative demand of the earthquake ground motions in the near source. *Earthquake engineering and structural dynamics*, **32**, 1853-1865, 2003.

[8] G. Manfredi, Evaluation of seismic energy demand. *Earthquake engineering and structural dynamics*, **30**, 485-499, 2001.

[9] S.K. Kunnath, Y.H. Chai, Cumulative damage-based inelastic cyclic demand spectrum. *Earthquake engineering and structural dynamics*, **33**, 499-520, 2004.

[10] S. Pampanin, G.M. Calvi, M. Moratti, Seismic behavior of R.C. beam-column joints designed for gravity loads. *12th European Conference on Earthquake Engineering*, London, UK, September 9-13, 2002.

[11] C. Fernandes, J. Melo, H. Rodrigues, A. Costa, H. Varum, A. Arede, Cyclic behaviour analysis of RC elements with plain reinforcing bars. *14th European Conference on Earthquake Engineering*, Ohrid, Macedonia 30 August – 03 September, 2010.

[12] G.M. Calvi, G. Magenes, S. Pampanin, Experimental test on a three storey r.c. frame designed for gravity only. *12th European Conference on Earthquake Engineering*, London, UK, September 9-13, 2002.

[13] A.C. Barrera, J.L. Bonet, M.L. Romero, P.F. Miguel, Experimental tests of slender reinforced concrete columns under combined axial load and lateral force. *Engineering Structures*, **33**(12), 3676–3689, 2011.

[14] EN 10080:2005, Steel for the reinforcement of concrete - Weldable reinforcing steel – General, European Committee for Standardization – CEN, 2005.

[15] UNE 36065 EX:2000, Norma Espanõla Experimental 2000 – Barras corrugadas de acero soldable con caracteristìcas especiales de ductilidad para armaduras de horigòn armado, 2000.

[16] LNEC E455-2008 – Varoes de aço A400 NR de ductilidade especial para armaduras de betão armado: caracteristìcas, ensaios e marcação, 2008.

[17] J.B. Mander, F.D. Panthaki, A. Kasalanati, Low-cycle fatigue behaviour of reinforcing steel. *Journal of Materials in Civil Engineering,* **6**(4), 453-468, 1994.

[18] J. Brown, SK. Kunnath, Low-Cycle Fatigue Failure of Reinforcing Steel Bars. *ACI Materials Journal*, **101**(6), 457-466, 2004.

[19] P. Crespi, Monotonic and cyclic behaviour of rebars in the plastic hinge of r.c. beams. PhD Thesis, 2002.

[20] C.A. Apostolopoulos, Mechanical behavior of corroded reinforcing steel bars S500s tempcore under low cycle fatigue. *Construction and Building Materials*, **21**, 1447–1456, 2006.

[21] UNI EN 1992-1-1:2005, Eurocode 2 (Annex C) - Design of concrete structures - Part 1-1: General rules and rules for buildings, 2005.

[22] C.A. Apostolopoulos, C. Ascanio, L. Bianco, A. Braconi, S. Caprili, G. Diamantogiannis, G. Ferreira Pimenta, M. Finetto, J. Moersch, W. Salvatore, Effects of corrosion on low-cycle fatigue (seismic) behaviour of high strength steel reinforcing bars. RFSR-CT-2009-00023 project. Final report, European Commission, Brussels, 2013.

[23] Mazzoni S, McKenna F, Scott MH, Fenves GL et al. (2007) OpenSees Command Language Manual, University of California, Berkley, USA.

[24] V. Ciampi, R. Eligenhausen, E.P. Popov, V.V. Bertero, Analytical Model tor Deformed Bar Bond under Generalized Excitations. Report EERC 82-23, Earthquake Engineering Research Center, University of California, Berkley, 1993.

[25] F. Braga, R. Gigliotti, M. Laterza, M. D'Amato, S. Kunnath, Modified Steel Bar Model Incorporating Bond-Slip for Seismic Assessment of Concrete Structures. *Journal of Structural Engineering*, **138**, 1342-1350, 2012.

[26] S. Hakuto, R. Park, H. Tanaka, Effect of deterioration of bond of beam bars passing through interior beam-column joints on flexural strenght and ductility. *ACI Structural Journal*, **96**(S94), 858-864, 1999.

[27] S. Caprili, Analysis of the low-cycle fatigue behaviour and corrosion phenomena on reinforcing bars of concrete structures in earthquake prone areas. PhD Thesis, University of Pisa, 2012.

[28] A. Braconi, F. Braga, S. Caprili, R. Gigliotti, W. Salvatore, Influence of low-cycle fatigue and corrosion phenomena on the structural behaviour of steel reinforcing bars. *15th World Conference on Earthquake Engineering*, Lisbon, Portugal, September 24-28, 2012.

[29] T.B. Panagiotakos, M.N. Fardis, Deformations of Reinforced Concrete Members at Yielding and Ultimate. *ACI Structural Journal*, **98**(2),135-148, 2001.

[30] F. Braga, R. Gigliotti, M. Laterza, Analytical Stress–Strain Relationship for Concrete Confined by Steel Stirrups and/or FRP Jackets. *Journal of Structural Engineering*, **132**, 1402-1416, 2006.

[31] CEB-FIP Model Code 1990 Design Code (1993), Comitè Euro-International du Beton.

[32] M. D'Amato, F. Braga, R. Gigliotti, M. Laterza, S. Kunnath, Validation of a Modified Steel Bar Model Incorporating Bond-Slip for Seismic Assessment of Concrete Structures. *Journal of Structural Engineering*, **138**, 1351-1360, 2012.

[33] A. Braconi, F. Braga, S. Caprili, R. Gigliotti, W. Salvatore, Seismic demand on steel reinforcing bars in reinforced concrete frame structures. Bulletin of Earthquake Engineering, under review, 2013.

[34] UNI EN 1998-3:2005, Eurocode 8 - Eurocode 8 - Design of structures for earthquake resistance - Part 3: Assessment and retrofitting of buildings, 2005.

[35] EN ISO 15630-1:2010, Steel for the reinforcement and prestressing of concrete - Test methods - Part 1: Reinforcing bars, wire rod and wire, 2010.